Ethanol stress induces transient restructuring of the yeast genome yet stable formation of Hsf1 transcriptional condensates

Linda S. Rubio, Suman Mohajan, David S. Gross*
Department of Biochemistry and Molecular Biology
Louisiana State University Health Sciences Center
Shreveport, LA 71130

*Corresponding author: david.gross@lsuhs.edu

Keywords: heat shock response; Heat Shock Factor (Hsf1); 3D genome; transcriptional condensates; chromatin; proteotoxicity; ethanol stress; RNA Pol II; *Saccharomyces cerevisiae*

Graphical Abstract

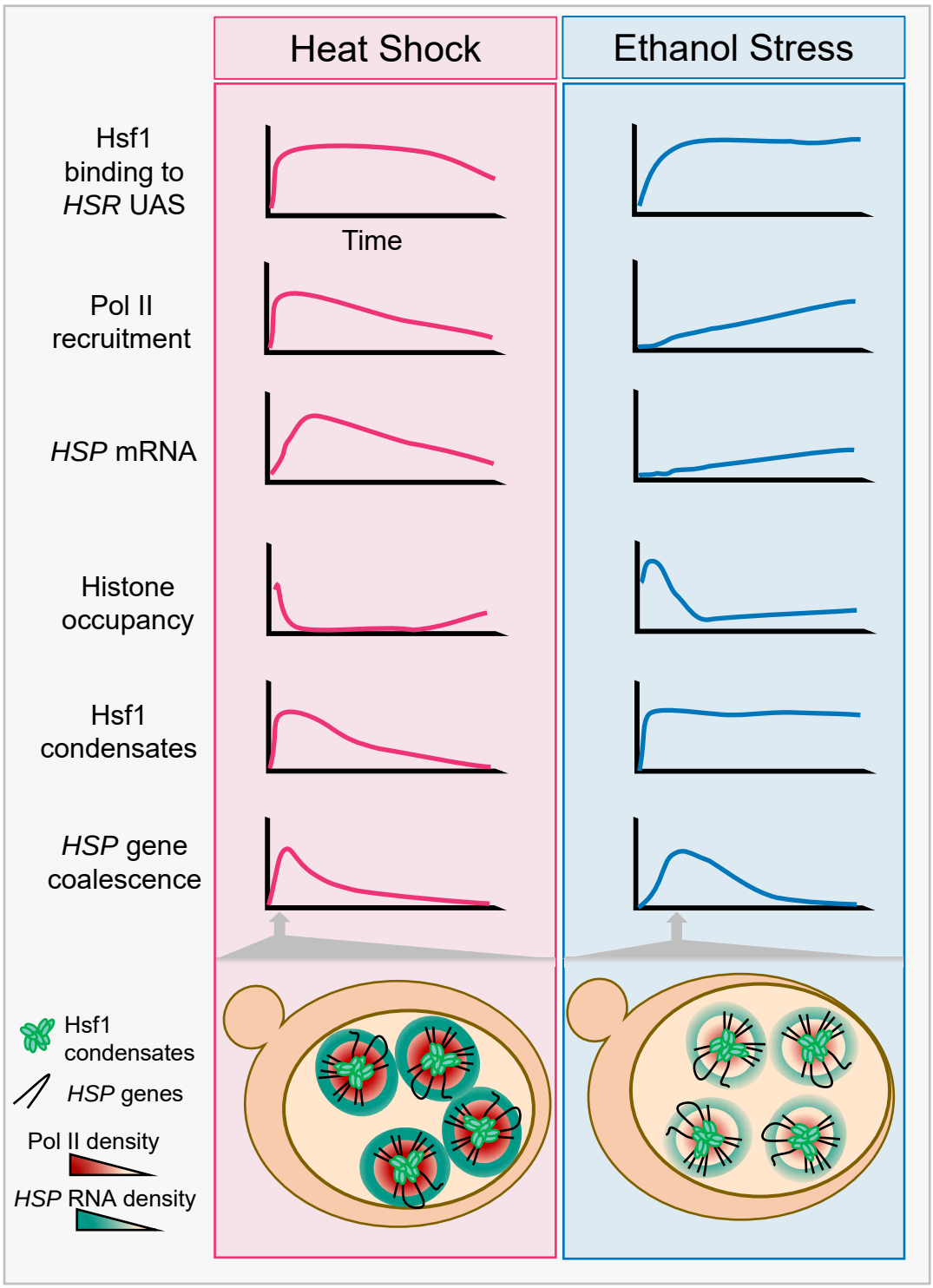

Abstract

In mammals, 3D genome topology has been linked to transcriptional states yet whether this link holds for other eukaryotes is unclear. Here we show that in budding yeast, *Heat Shock Response* (*HSR*) genes under the control of Heat Shock Factor (Hsf1) rapidly reposition in cells exposed to acute ethanol stress and engage in concerted, Hsf1-dependent intergenic interactions. Accompanying 3D genome reconfiguration is equally rapid formation of Hsf1-containing condensates. However, in contrast to the transience of Hsf1-driven intergenic interactions that peak within 10 min and dissipate within 1 h, Hsf1 condensates are stably maintained for hours. Moreover, under the same conditions, Pol II occupancy of *HSR* genes and RNA expression are detectable only later in the response and peak much later (>1 h). This contrasts with the coordinate response of *HSR* genes to thermal stress where Pol II occupancy, transcription, intergenic interactions, and formation of Hsf1 condensates are all rapid yet transient (peak within 2.5-10 min and dissipate within 1 h). Collectively, our data suggest that different stimuli drive distinct transcription, topologic, and phase-separation phenomena dependent on the same transcription factor and that transcription factor-containing condensates represent only part of the ensemble required for gene activation.

Introduction

Genomes of higher eukaryotes are organized into multiple hierarchical levels. Chromosomes are segregated within individual territories, and within chromosomal territories active and inactive regions are separated into topologically associated domains (TADs) (Wendt & Grosveld, 2014). Within TADs, DNA loops are formed to permit the interaction between enhancers or silencers and the promoters of their target loci. Although this hierarchy suggests a static view of the genome, recent studies have revealed that the genome is dynamic, as multiple points of interaction form in response to developmental cues and other stimuli. This dynamic restructuring ranges from the interactions between co-regulated genes (Fanucchi et al., 2013; Papantonis et al., 2012; Park et al., 2014; Schoenfelder et al., 2010) to the convergence of enhancers dispersed across multiple chromosomes into a hub that regulates a single gene (Monahan & Lomvardas, 2015) to the reorganization of the genome that occurs in the zygote (Schulz & Harrison, 2019).

Despite its evolutionary distance, the yeast *Saccharomyces cerevisiae* also possesses an organized genome. Centromeres are located in a cluster at the spindle pole body, while chromosomal arms are extended with telomeres and the nucleolus located at the opposite side of the nucleus (Duan et al., 2010), resulting in a Rabl-like configuration (Taddei & Gasser, 2012). And as in higher eukaryotes, the budding yeast genome is organized into TAD-like structures (Eser et al., 2017) subdivided into smaller loop domains (Hsieh et al., 2015). Also as is the case in mammalian cells, the yeast genome is not static. Genes, including *INO1, GAL1* and *GAL10*, have been observed to reposition from the nuclear interior to the nuclear periphery upon their activation (Brickner et al., 2019; Brickner & Walter, 2004; Cabal et al., 2006; Casolari et al., 2004; Dieppois et al., 2006; Green et al., 2012). Even more dramatic are *Heat Shock Response* (*HSR*) genes under the regulation of Heat Shock Factor (Hsf1). Upon exposure to acute thermal stress (heat shock), *HSR* genes dispersed across multiple chromosomes transcriptionally activate and engage in novel *cis*- and *trans*-intergenic interactions between one another, culminating in their coalescence into intranuclear foci

(Chowdhary et al., 2017, 2019). These stress-induced foci, comprised of Hsf1 and components of the transcriptional machinery, exhibit properties of liquid-liquid phase-separated condensates (Chowdhary et al., 2022). Hsf1 condensate formation elicited by heat shock, like that of *HSR* gene coalescence, parallels the kinetics of induction and attenuation of Hsf1-dependent genes (Chowdhary et al., 2017).

The Hsf1-driven heat shock response is a fundamental, evolutionarily conserved transcriptional program characterized by the gene-specific transcription factor (TF) Hsf1, its DNA recognition element (heat shock element (HSE)) and a core set of target genes encoding molecular chaperones and co-chaperones (reviewed in (Verghese et al., 2012)). In absence of proteotoxic stress, yeast Hsf1 is bound by Hsp70 and its co-chaperone Sis1 in the nucleoplasm (Feder et al., 2021; Krakowiak et al., 2018; Peffer et al., 2019; Zheng et al., 2016). Upon encountering stress, Hsp70 is titrated by unfolded proteins, particularly orphan ribosomal proteins located in the nucleolus and nascent polypeptides in the cytosol (Albert et al., 2019; Ali et al., 2022; Tye et al., 2019; Tye & Churchman, 2021), resulting in the release of Hsf1 which then trimerizes and binds to HSEs located upstream of ~50 genes whose activation is dependent on this factor (Pincus et al., 2018). Once proteostasis is reestablished, excess Hsp70 binds Hsf1, inactivating it, thereby closing the negative feedback loop that regulates Hsf1 transcriptional activity.

In addition to thermal stress, Hsf1 can be activated by chemical stressors such as ethanol. Ethanol is a metabolite of glucose breakdown that budding yeast cells secrete into their surroundings. Ethanol production helps yeast outcompete other microbes in the environment (Liti, 2015; Piškur et al., 2006; Rozpedowska et al., 2011). Once glucose is depleted, ethanol serves as an alternative carbon source (Piškur et al., 2006). Given this strategic use of ethanol, it is of fundamental importance for yeast to have a mechanism in place to respond to the stress that ethanol elicits. Similar to thermal stress, exposure to ethanol causes a large number of cellular perturbations including disruption of the plasma membrane (Piper et al., 1994); disruption of the H^+ ATPase and intracellular acidification (Rosa & Sá-Correia, 1991, 1996; Triandafillou et

al., 2020); production of reactive oxygen species (Bandas & Zakharov, 1980; Davidson et al., 1996); depolymerization of the actin cytoskeleton (Homoto & Izawa, 2018; Tan et al., 2017); cell cycle arrest (Johnston & Singer, 1980; Kubota et al., 2004); disruption of mRNP transport to the daughter cell and formation of stress granules (Grouši et al., 2009; Kato et al., 2011); global inhibition of transcription and translation (Bresson et al., 2020; Gasch et al., 2000); and formation of protein aggregates (Piper, 1995; Plesset et al., 1982; Stanley et al., 2010). The cell counteracts many of these perturbations through the production of molecular chaperones.

Here, we investigate activation of the HSR in yeast exposed to ethanol stress (ES) and compare it to the response induced by heat shock (HS). We find that similar to HS, exposure to ES induces transcription of Hsf1-regulated genes and elicits concerted intergenic interactions between them (*HSR* gene coalescence). In contrast to HS, however, intergenic interactions in ES-induced cells peak well before transcription. Likewise, in response to ES, Hsf1 condensate formation precedes transcriptional activation as its onset parallels that of *HSR* gene coalescence. Cytosolic protein aggregation exhibits similar rapid kinetics as *HSR* gene coalescence and Hsf1 condensate formation. The delay in transcriptional induction may be linked to profound chromatin compaction that occurs upon exposure of cells to ethanol, a condition that correlates with suppressed displacement of histones during transcription. At longer times of ethanol exposure, *HSR* gene transcript accumulation continues to increase while *HSR* gene coalescence has already dissipated. Likewise, ES-induced Hsf1 condensates are present for ≥2.5 h, in contrast to HS-induced condensates that begin to dissipate within 30 min. Collectively, our data indicate that different stimuli drive distinct transcription, chromatin, topologic and phase-separation phenomena, yet all are dependent on Hsf1.

Results

Ethanol stress induces transcriptional activation of Hsf1-dependent genes but with delayed kinetics and reduced expression versus thermal stress

Saccharomyces cerevisiae in the wild metabolizes glucose and other sugars into ethanol, which the yeast secretes into the environment to suppress microbial competition. Therefore, it is likely that yeast has evolved mechanisms to contend with ethanol toxicity. Indeed, a common laboratory strain (W303) retains viability when cultivated in the presence of a relatively high concentration of ethanol (8.5%), although its ability to proliferate is diminished (**Figure 1A, B**). As assessed by the presence of Hsp104-containing foci (a measure of protein aggregation (Liu et al., 2010)), the rate of cytosolic protein aggregation is similar in ethanol- and thermally stressed cells (**Figure 1D,E**; see **Figure 1C** for experimental design). However, it is notable that the extent of Hsp104 foci, and by extension protein aggregation, is substantially higher in cells subjected to ethanol stress.

To gain insight into the mechanism by which *S. cerevisiae* contends with ethanol-induced proteotoxicity, we assessed the kinetics of transcriptional activation of *HSR* genes in cells exposed to ethanol stress. Cells were cultivated to early log phase in rich YPD medium, then ethanol was added to a final concentration of 8.5% and cell aliquots were removed at 0, 10, 20 and 60 min. Transcription was terminated through addition of sodium azide (Lee & Garrard, 1991) (see Materials and Methods). A parallel culture was exposed to an instantaneous 30° to 39°C heat shock and cells were removed at the corresponding time points. Transcription was terminated as above.

While cells exposed to heat shock displayed a rapid and substantial increase in *HSR* gene expression (typically >10-fold increase in RNA levels within 10 min of thermal upshift), those exposed to ethanol stress only weakly induced the same cohort of genes (**Figure 2A**). However, while HS induced a transient increase in RNA expression, ES induced a sustained increase that was evident at all Hsf1-dependent genes tested (**Figure 2–figure supplement 1**). In the case of *HSP12*, whose transcription is under

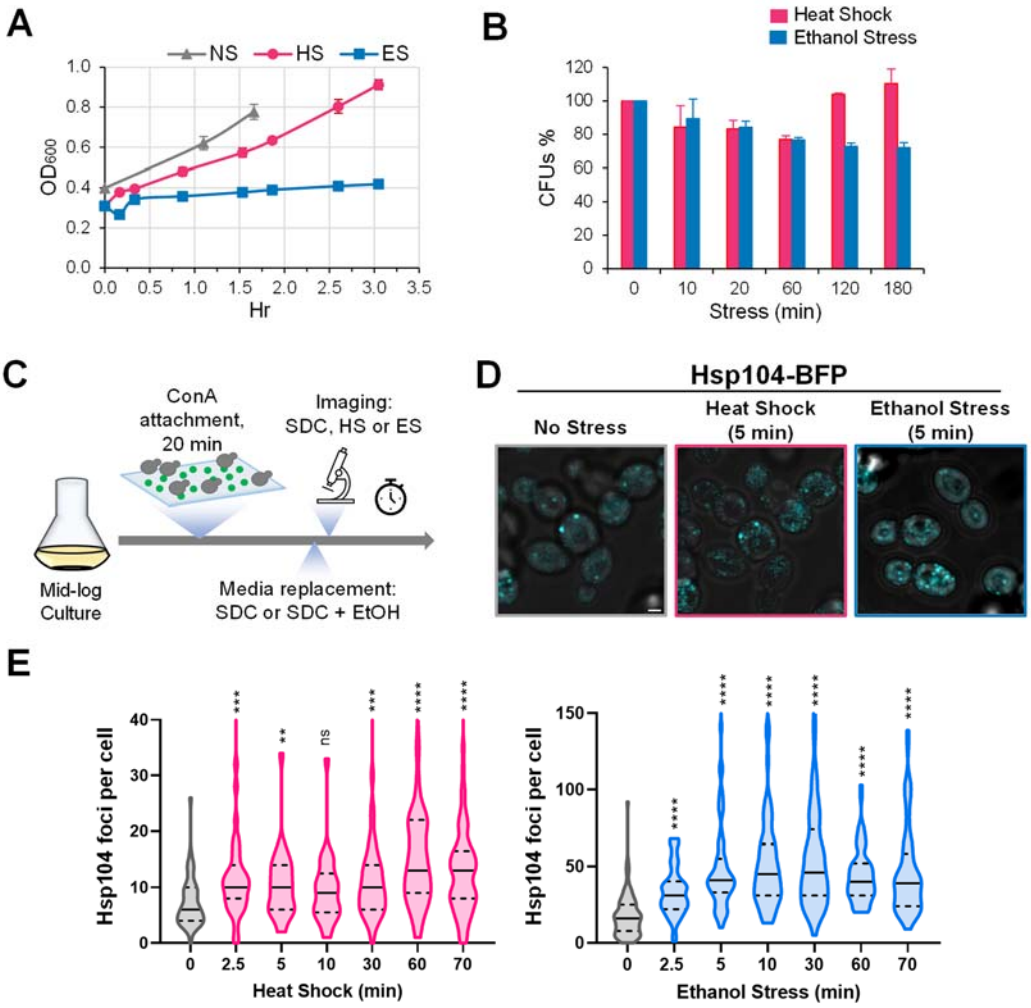

Figure 1. Ethanol stress induces extensive protein aggregation

(A) Growth curve of strain W303-1B grown in liquid culture (YPDA). Mid-log phase cultures were diluted to A_{600} =0.4 and shifted to different conditions: no stress (NS, 25°C), heat shock (HS, 39°C), or ethanol stress (ES, 8.5% v/v, 25°C). A_{600} was monitored over time. Means and SD are shown. N=2.

(B) Viability assay of W303-1B cells following exposure to heat shock or ethanol stress. An aliquot was taken from each condition at the listed stress timepoints and diluted in rich media. Cells were spread on YPDA plates and grown at 30°C for 3 days. Colony forming units (CFUs) were determined using ImageJ/FIJI. Plotted are percentages of stressed cells normalized to the 0 min control. Graphs depict means + SD. N=2.

(C) Experimental strategy for imaging Hsp104 foci. Cells were attached to a concanavalin A (ConA)-coated surface, followed by heat shock or ethanol stress treatment (see Materials and Methods). Synthetic complete media (SDC) was supplemented with ethanol to a final concentration of 8.5% for ES samples. Scale bar: 2 µm.

(D) Both heat shock and ethanol stress induce formation of Hsp104 foci. LRY033 cells were maintained at 25°C (no stress) or exposed to either 39°C heat shock or 8.5% ethanol stress. Hsp104-BFP foci were visualized by confocal microscopy. Shown are maximal projections of 11 z-planes, taken with 0.5 µm of interplanar distance. Scale bar: 2 µm.

(E) Cells subjected to the above treatments were assayed for Hsp104 puncta. An average of 40 cells per timepoint, per condition, was quantified using Imaris software (v.10.0.0). Significance was determined by Mann Whitney test. ****, $p<0.0001$; ***, $p<0.001$; **, $p<0.01$; *ns,* not significant.

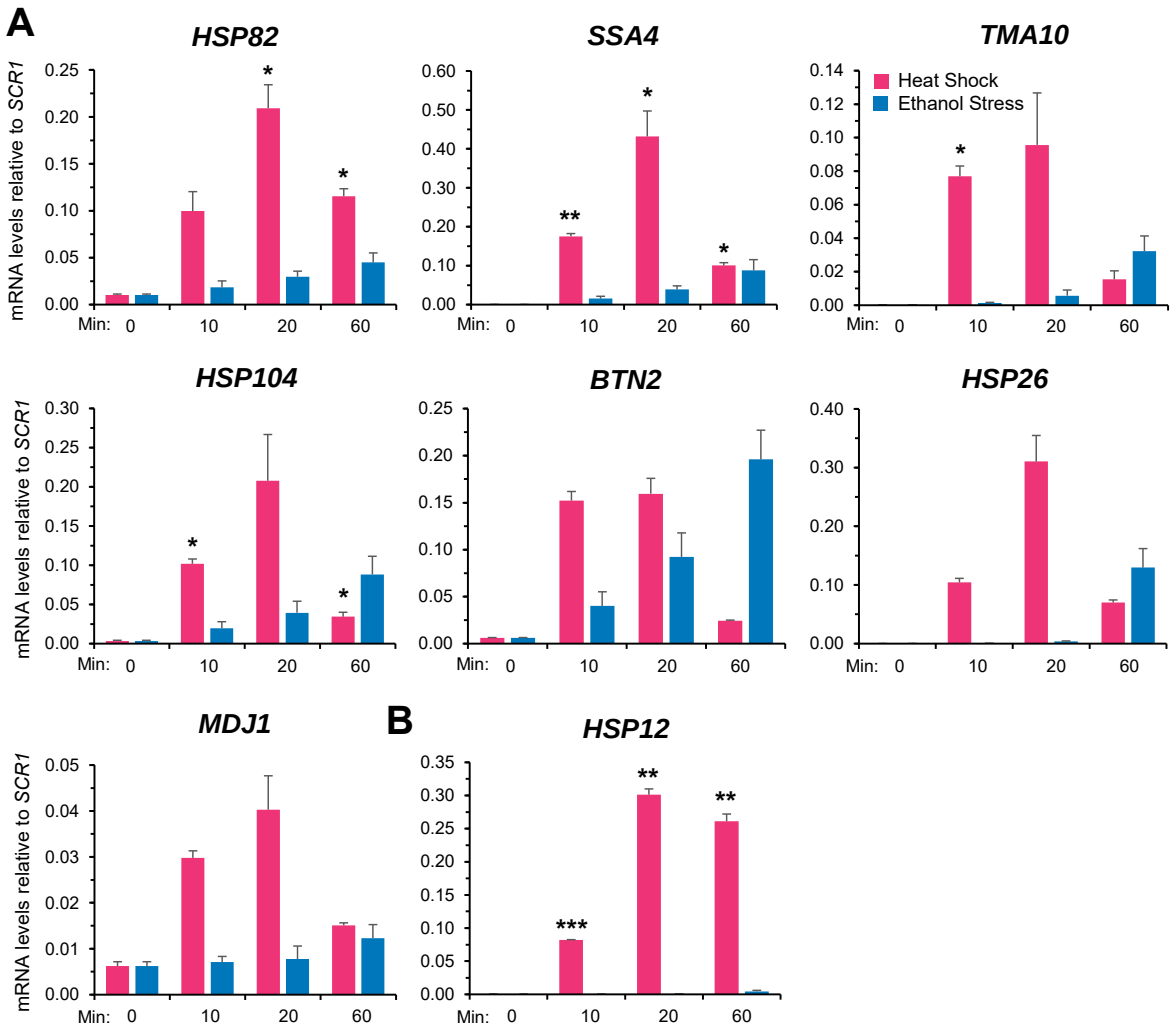

Figure 2. Ethanol stress transcriptionally induces Hsf1-dependent genes but with markedly slower kinetics than thermal stress

(A) RNA abundance of *Heat Shock Response* (*HSR*) genes was determined by Reverse Transcription-qPCR in strain W303-1B. Heat shock was performed at 39°C; ethanol stress was done using 8.5% (v/v) ethanol at 25°C. Depicted are means + SD. N=2, qPCR=4. Statistical analysis: T-test, one-tailed, unequal variance, no stress vs stress conditions. *, $p<0.05$; **, $p<0.01$.

(B) As in (A), but the Hsf1-, Msn2-dual regulated gene *HSP12* was evaluated. ***, $p<0.001$.

the dual regulation of Msn2 and Hsf1, exposure to heat shock resulted in a high level of induction as previously observed (Chowdhary et al., 2019) yet exposure to 8.5% ethanol failed to cause detectable activation (**Figure 2B**). Nonetheless, as described below, *HSP12* responds to ethanol stress but does so through its inducible and dramatic 3D genomic repositioning.

Pol II recruitment and histone eviction are likewise delayed in ethanol-stressed cells and this correlates with transient, widespread increase in nucleosome density

The delayed transcriptional response of *HSR* genes in ES- vs. HS-treated cells prompted us to investigate occupancy of Hsf1, RNA Pol II and histones at these genes over a time course. A possible explanation for the delay in activation in cells exposed to ethanol stress is reduced Hsf1 binding to the genes' upstream regulatory regions. To explore this possibility, we exposed cells to either thermal or chemical stress and processed them for chromatin immunoprecipitation (ChIP) analysis. As previously observed (Kim & Gross, 2013; Pincus et al., 2018; Sekinger & Gross, 2001), occupancy of Hsf1 at its target loci increases at least several-fold following a brief heat shock (**Figure 3B,** left, dark red; see **Figure 3A** for location of primers). Factor occupancy typically declines after 60 min of continuous thermal stress and in the case of *TMA10*, dissociation begins much sooner. In response to ethanol stress, Hsf1 occupancy steadily increased, in most cases reaching maximal levels by 20 min and plateauing thereafter (**Figure 3B,** left, black). These results suggest that ethanol stress induces binding of Hsf1 to HSEs to a degree similar to heat shock, yet such binding is more gradual. Moreover, Hsf1's chromatin binding fails to elicit a corresponding transcriptional response given the results discussed above.

In light of this disconnect between Hsf1 binding and *HSR* mRNA production, we evaluated abundance of the Rpb1 subunit of Pol II at representative genes over the same time course. In response to heat shock, Pol II is rapidly recruited to the promoters and coding regions of each *HSR* gene, peaking within 2.5 min and then gradually declining over the next ~60 min (**Figure 3B**, middle, red and pink traces). By contrast,

Pol II occupancy is noticeably delayed in cells exposed to ethanol stress (**Figure 3B**, middle, blue traces), consistent with reduced transcript levels (**Figure 3–figure supplement 1B**). The increase in *HSR* mRNA in heat-shocked cells parallels, yet consistently lags, the abundance of Pol II within *HSR* gene coding regions (**Figure 3–figure supplement 1A**). This delay in reaching peak accumulation may reflect contributions beyond RNA synthesis, such as transient enhanced stability of *HSR* transcripts during the acute phase of heat shock.

To obtain further insight into the chromatin landscape present during the two stresses, we assayed histone H3 abundance as a measure of nucleosome density. In response to heat shock, nucleosomes are rapidly displaced over the promoter, coding and 3'-flanking regions of strongly expressed *HSR* genes (*HSP82, HSP104 and SSA4);* a similar, albeit delayed, response is observed for *TMA10* and *HSP12*. Following this initial phase (~20 min), nucleosomes reassemble over all four genes, often returning to their original density by 60 min (**Figure 3B**, right, red and pink traces). This dramatic and dynamic remodeling has been previously observed (Kremer & Gross, 2009; Zhao et al., 2005). In contrast, ethanol stress elicits a transient increase in nucleosome density over all five genes (**Figure 3B**, right, blue traces). This apparent increase in chromatin compaction is not restricted to *HSR* genes; a variety of unrelated loci, including a stress-responsive, Msn2-regulated gene (*PGM2*), two constitutively expressed genes (*TUB1, ACT1*), two genes assembled into *SIR*-dependent heterochromatin (*HMLα1, YFR057w*) and a non-transcribed region (*ARS504*) also exhibit a transient increase in nucleosome density in ethanol-exposed cells (**Figure 3–figure supplement 2A**). These data suggest that the increase in nucleosome density antagonizes Pol II recruitment and its subsequent release into the coding regions of *HSR* genes.

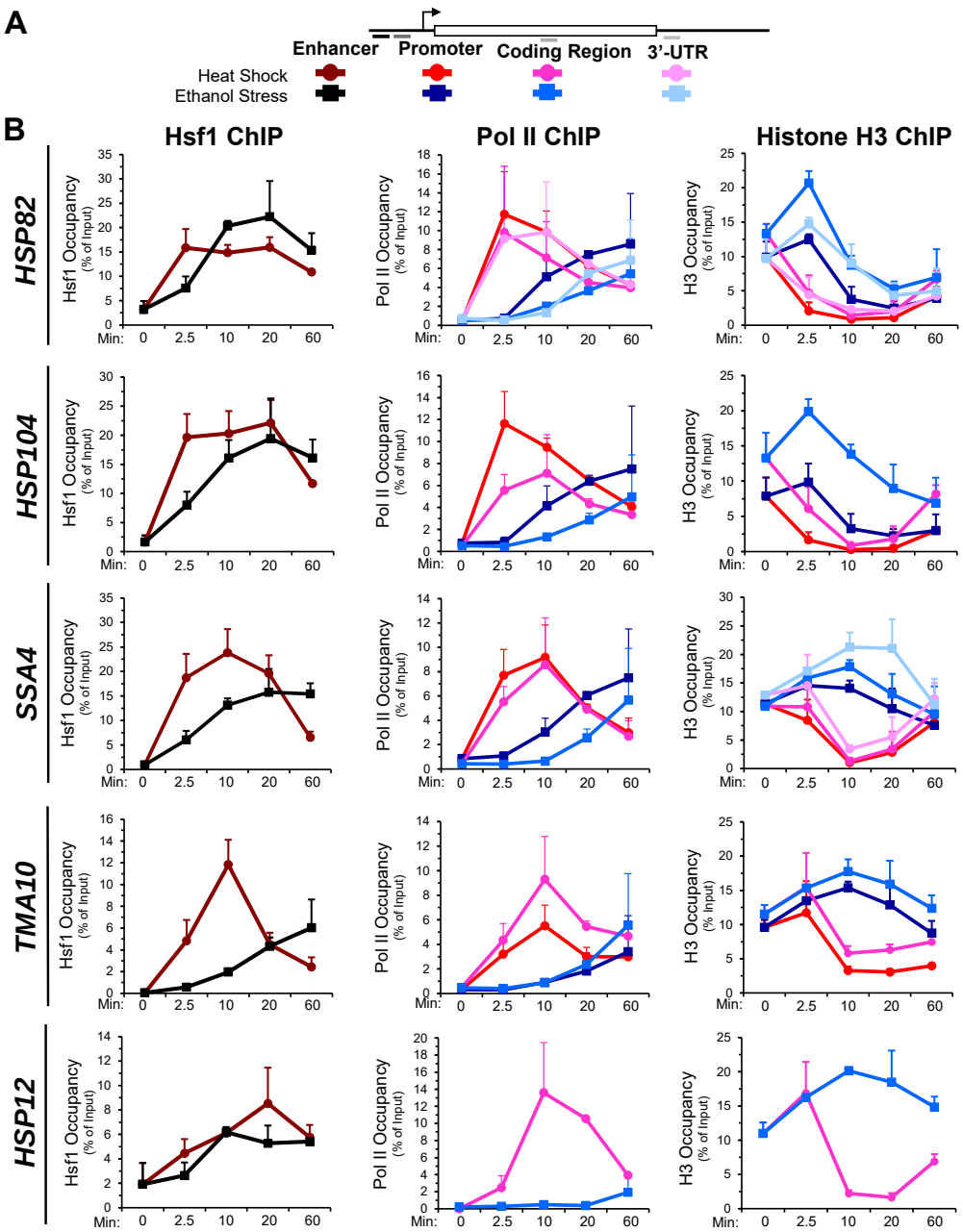

Figure 3. Hsf1 and Pol II recruitment is delayed while histone occupancy transiently increases at *HSR* genes in ethanol stressed cells

(A) Map of a representative *HSR* gene depicting locations of primers used for chromatin immunoprecipitation (ChIP) analysis. Heat shock: shades of red and pink. Ethanol stress: shades of blue.

(B) ChIP analysis of Hsf1, Pol II (Rpb1) and histone H3 occupancy at different loci within the indicated *HSR* genes. Mid-log cultures of strain BY4741 were subjected to the indicated times of heat shock (39°C) or ethanol stress (8.5% v/v, 25°C). Antibodies raised against full-length Hsf1, CTD of Rbp1 or the globular domain of Histone H3 were used (see Materials and Methods). ChIP signals were normalized to input. Shown are means + SD. N=2, qPCR=4.

To provide an orthogonal line of evidence for increased chromatin compaction, we used a strain that expresses a histone H2A-mCherry fusion and measured the change in H2A-mCherry volume by live cell fluorescence microscopy. Consistent with ChIP, exposure to ethanol stress induced a sustained decrease in chromatin volume between 2.5 - 60 min (**Figure 3–figure supplement 2B, 2C**), suggesting that yeast responds to ethanol stress by compacting its genome. A similar but more transient decrease in chromatin volume is seen in cells exposed to acute thermal stress (**Figure 3–figure supplement 2B, 2C**), consistent with the transient increase in H3 abundance at loci such as *TMA10* and *HSP12* (**Figure 3**). Why H3 occupancy increases at *TMA10* and *HSP12* yet not at other *HSR* genes could be related to their modest rate of transcription during the first few minutes of HS (Pincus et al., 2018). Altogether, our ChIP data indicate that Hsf1 binds to its target enhancers less readily in ethanol-stressed than in thermally stressed cells. This impediment to Hsf1 occupancy is magnified by a corresponding, and more severe, hindrance to Pol II recruitment resulting in a pronounced delay in *HSR* gene transcription.

Acute ethanol stress induces rapid and profound 3D genomic repositioning of *HSR* loci

An intriguing feature of *HSR* genes is the fact that they coalesce into discrete intranuclear foci in response to heat shock. Such interactions have been documented using both molecular (chromosome conformation capture (3C)) and imaging (fluorescence microscopy) approaches (Chowdhary et al., 2017, 2019, 2022). Intriguingly, physical interactions specifically involve Hsf1 targets irrespective of their location in the genome. Other loci, including adjacent, transcriptionally active genes, show little or no tendency to interact with Hsf1-dependent genes. Such *cis*- and *trans*-interactions involve regulatory as well as coding regions and are highly dynamic, typically peaking at 2.5 min and dissipating by 30-60 min. The kinetics of coalescence often, although not always, correlate with kinetics of transcriptional induction; they also parallel the formation of Hsf1 condensates as discussed further below (Chowdhary et al., 2017, 2019, 2022).

Given these previous observations, we wished to know if ethanol stress induced a similar 3D genome restructuring. It seemed unlikely that such topological changes would occur during the initial phase of ES since only weak Pol II occupancy and *HSR* gene transcription are observed as described above (**Figures 2, 3**). However, as shown in **Figure 4**, ES triggered frequent intergenic interactions between Hsf1 targets during the first 10 min as revealed by TaqI-3C, a highly sensitive, quantitative version of 3C (Chowdhary et al., 2020) (see **Figure 4 – figure supplement 1** for location of 3C primers). Both intra- and interchromosomal interactions are present. Moreover, the interaction frequencies following this exposure in most cases equaled, and in some instances exceeded, those detected in cells heat-shocked for 2.5 min (**Figures 4A, 4B**), when peak 3C interactions occur in thermally stressed cells (Chowdhary et al., 2017). A detailed kinetic analysis revealed that intergenic interactions elicited by ethanol stress, similar to those elicited by thermal stress, are highly dynamic: detectable within 2.5 min, peak shortly thereafter (within 10 min) and largely attenuate by 60 min (**Figure 5A** and (Chowdhary et al., 2017)).

It has been previously suggested that a functional link exists between gene looping and transcriptional activation (Ansari & Hampsey, 2005; O'Sullivan et al., 2004). Indeed, gene loops and other intragenic 'crumpling' interactions (Chowdhary et al., 2017) are readily detected within *HSR* genes in cells exposed to ethanol. However, as is the case with intergenic interactions, these topological changes are kinetically uncoupled from both transcription and Pol II occupancy: they are detectable within 2.5 min, peak at 10 min and return to basal levels by 60 -120 min (**Figure 5B** and **Figure 4 – figure supplement 2**). Taken together, our 3C and expression analyses indicate that 3D genomic repositioning and intragenic looping of *HSR* genes precedes the maxima of transcription and Pol II occupancy. Moreover, for certain loci (e.g., *HSP12*), they argue that even a minimal level of transcription and Pol II recruitment is not required to drive 3D topological changes in these genes.

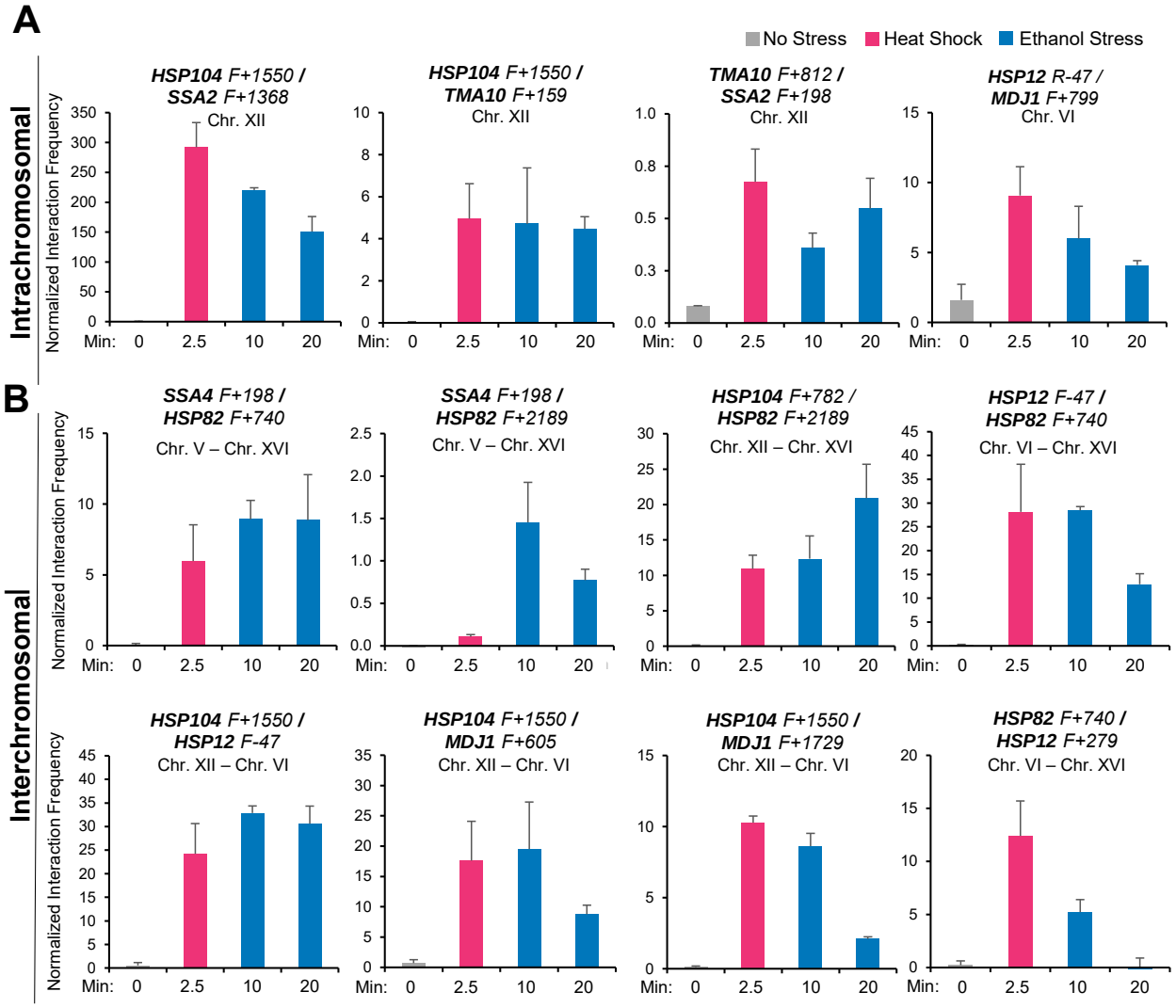

Figure 4. Ethanol stress induces intergenic interactions between *HSR* genes that are as frequent as those induced by acute thermal stress

(A) Intrachromosomal *(cis)* interactions between *HSR* genes were analyzed by TaqI-3C. W303-1B cells were instantaneously shifted from 30° to 39°C for 2.5 min (heat shock (HS)) or exposed to 8.5% v/v ethanol at 25°C for 10 or 20 min (ES). No stress samples were kept at 25°C. Location of TaqI coordinates are provided in Figure 4–figure supplement 1. F (forward) primers are positioned near the indicated TaqI restriction site. 3C signals were normalized to the 3C signal derived from using a naked genomic DNA template. Graphs depict means + SD; N=2; qPCR=4.

(B) Interchromosomal *(trans)* interactions between *HSR* genes performed as in (A).

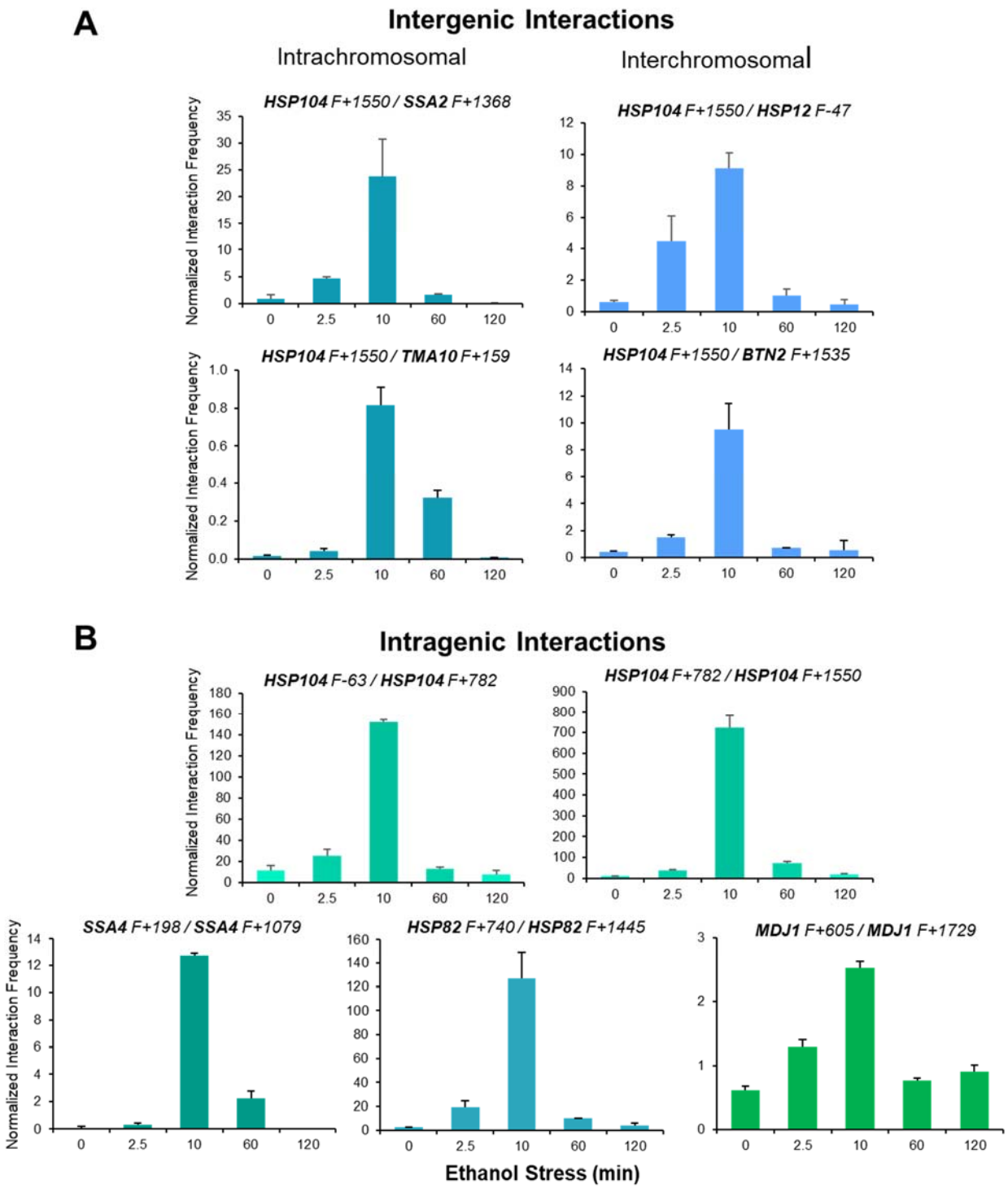

Figure 5. Ethanol-induced *HSR* gene interactions are detectable by 2.5 min but typically dissipate within 60 min

(A) TaqI-3C analysis of intergenic interactions occurring during ethanol stress was conducted as described in Figure 4. All samples were kept at 25°C. Locations of TaqI restriction sites are provided in Figure 4–figure supplement 1. Data are plotted as means + SD. N=2, qPCR=4.

(B) As in (A), but for intragenic interactions (crumpling).

Live cell imaging reveals that *HSR* genes coalesce to a similar degree under ethanol- and heat-stress conditions

To provide an orthogonal line of evidence for *HSR* gene interaction, we employed fluorescence microscopy to image live cells bearing *LacO*-tagged *HSP104* and *TetO*-tagged *TMA10* loci in cells expressing LacI-GFP and TetR-mCherry fusion proteins. Both genes are located on Chromosome XII, on opposite arms, and are physically separated by the nucleolus (rDNA repeats) that lies between them (Duan et al., 2010) (schematically depicted in **Figure 6A**). In the absence of stress, fluorescence signals representing these two genes are typically well-separated (**Figure 6B**, 0 min). Upon heat shock, they rapidly converge, usually within 2.5 min. Upon exposure to ethanol, gene convergence is also observed, albeit less rapidly (**Figure 6B**; see also below). Despite the slight delay, these results demonstrate that *HSP104* and *TMA10* coalesce in ethanol stressed cells with similar frequency as in thermally stressed cells (**Figure 6C**), consistent with the 3C analysis above.

Having confirmed the physical interaction of Hsf1-dependent genes under ethanol stress, we assessed the transcriptional status of coalesced genes. Our RT-qPCR analysis indicated that the increase in *HSR* mRNA levels in ES-induced cells is delayed compared to those in HS-induced cells (**Figure 2**). To obtain insight into *HSR* gene transcription kinetics in single cells, we integrated a stem loop array (MS2x24) upstream of *HSP104*, allowing production of a chimeric transcript visualized upon binding of the MCP-mCherry fusion protein (schematically illustrated in **Figure 6D**) (Haim et al., 2007). This strain also harbored *LacO*-tagged *HSP104* and *HSP12* genes and expressed LacI-GFP. We were unable to detect an enhanced MCP-mCherry signal adjacent to *HSP104* under no stress conditions (**Figure 6E**), consistent with very low *HSP104* basal transcript levels (**Figure 2A**). Heat shock induced rapid coalescence between *HSP104* and *HSP12*, as well as transcription from *HSP104*. These phenomena were detectable by 2.5 min as a merged signal of the chimeric transcript and two GFP-labeled genes (**Figure 6E,** middle). This visualization method allowed us to quantify the percentage of the population that is actively engaged in transcription, revealing that during heat shock,

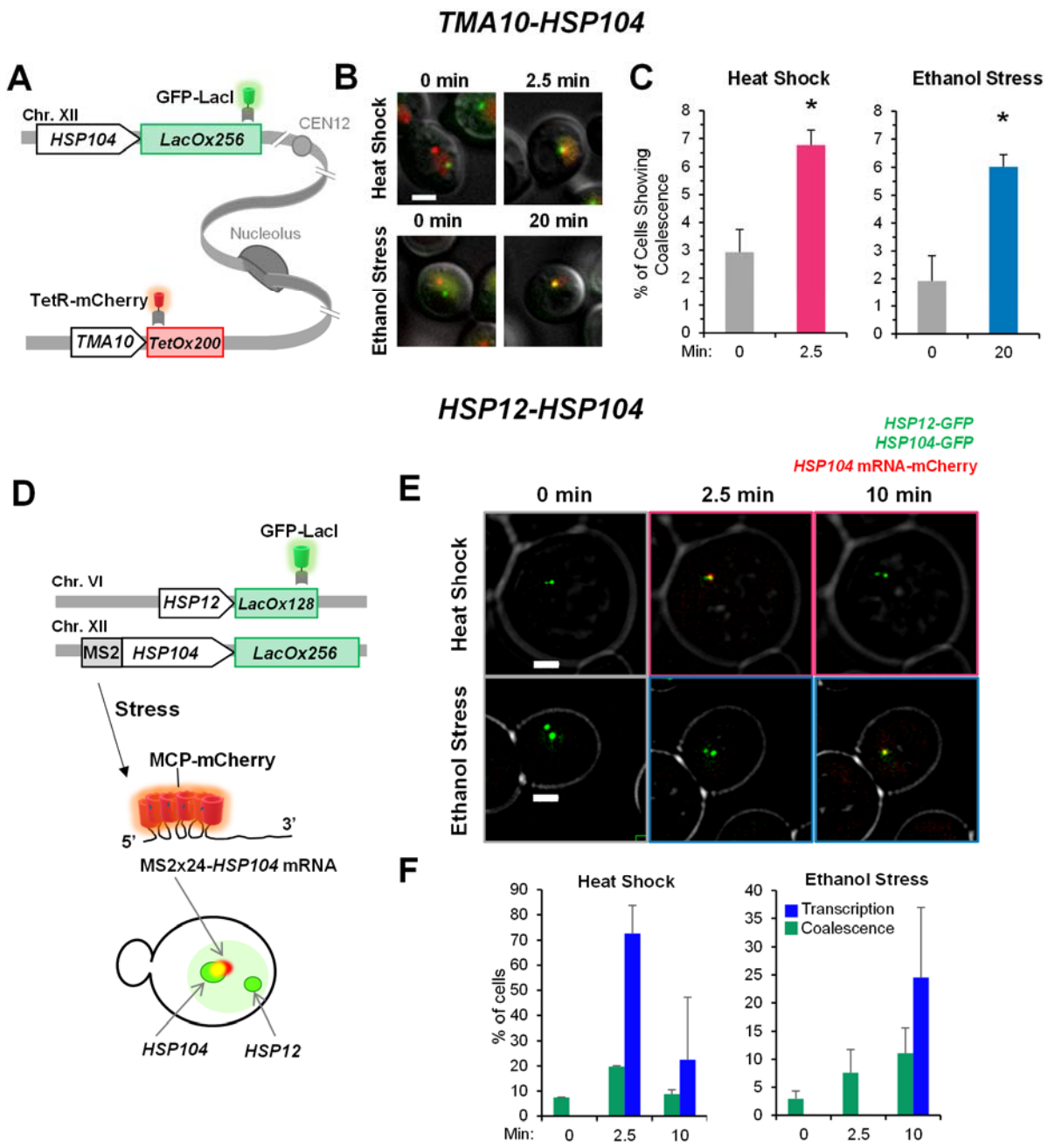

Figure 6. *HSR* genes coalesce in response to ethanol stress at a frequency comparable to that elicited by heat shock

(A) Relative location of *HSP104* and *TMA10* on Chr. XII in the diploid strain ASK727. As indicated, one allele of *HSP104* is flanked by an integrated $LacO_{256}$ array and one allele of *TMA10* is flanked by a $TetO_{200}$ array. ASK727 also expresses GFP-LacI and TetR-mCherry to allow visualization of the two genes as a green and red dot, respectively.

(B) Live cell widefield fluorescence microscopy of ASK727. Cells were immobilized onto ConA-coated coverslips and exposed to either heat shock (25°C to 38°C upshift) or ethanol stress (25°C, 8.5%) for the indicated times (see Materials & Methods). 11 z-planes with 0.5 µm interplanar distance were captured for each condition. A representative z-plane is shown per condition. Scale bar: 2 µm.

(C) ASK727 cells, treated as in B, were scored for colocalization of *HSP104* and *TMA10* upon exposure to either heat shock or ethanol stress. A cell was scored as positive when the highest intensity signal from both genes overlapped in the same z-plane. An average of 70 cells were evaluated per condition, per timepoint. Displayed are means + SD. N=2. One-tailed t-test was performed to assess significance. **, p<0.01. Note:* we interpret *HSP104-TMA10* coalescence observed at T=0 min to principally reflect coincidental overlap given absence of 3C signal under the no stress condition. A similar consideration applies to the *HSP104-HSP12* gene pair analyzed below.

(D) Chromosomal location of *HSP12* and *HSP104* and the *LacO* arrays flanking each in the diploid strain VPY705. *HSP104* has, in addition, a 24xMS2 loop array integrated within the 5'-UTR downstream of the endogenous promoter. Upon transcriptional activation of *HSP104*, MCP-mCherry binds to the nascent chimeric transcript and is visualized as a red dot adjacent to the gene (green dot).

(E) Live cell confocal fluorescence microscopy of strain VPY705 treated as in (B) for the indicated times but using an Olympus spinning disk confocal microscope system for imaging and a VAHEAT device for heat shock (39°C, see Materials & Methods). Scale bar: 2 µm.

(F) Quantification of VPY705 cells treated as above and scored for the coalescence of *HSP104-HSP12* and the presence of chimeric *MS2x24-HSP104* mRNA. Cells were scored positive for coalescence only when a single green dot could be visualized in the nucleus across the 11 z-planes. Transcription was scored as positive only when a signal above background could be seen for a red dot near the large green dot (*HSP104*). Approximately 40 cells were scored per timepoint, per condition. Graphs represent means + SD. N=2.

transcription and coalescence are positively correlated (**Figure 6F,** left). Consistent with this, after transcription declined (10 min HS), so did *HSP104-HSP12* coalescence.

A detailed single cell analysis supports the strong spatiotemporal correlation between *HSR* gene coalescence and transcription in heat-shocked cells (**Figure 6 – figure supplement 1**). In contrast, under ethanol stress, *HSP104* RNA was not detected in most cases until 10 min even though *HSP12* and *HSP104* coalesced as early as 2.5 min (**Figure 6F**). Indeed, a detailed single cell analysis reveals clear temporal uncoupling between *HSR* gene coalescence and *HSR* gene transcription in ethanol stressed cells (**Figure 6 – figure supplement 1**). Underscoring the disconnect between 3D genome repositioning and transcription is the fact that *HSP12* RNA was undetectable within ES-treated cells until 60 min (**Figure 2B and Figure 2 – figure supplement 1**). Collectively, our RT-qPCR, 3C and imaging data argue that ethanol stress induces striking topological changes in *HSR* genes and that these are accompanied by minimal transcriptional output. This provides a strong contrast to the case in heat-shocked cells where there exists a strong temporal correlation between *HSR* gene transcription and *HSR* gene repositioning.

Ethanol stress induces rapid formation of long-lived Hsf1 condensates

Recently, TF condensates have been proposed as a mechanism for transcriptional regulation (Boija et al., 2018; Cho et al., 2018; Hnisz et al., 2017; Nair et al., 2019; Sabari et al., 2018). Heat shock-activated Hsf1 phase separates in both human (Zhang et al., 2022) and budding yeast cells (Chowdhary et al., 2022), forming biomolecular condensates that correlate with *HSR* gene transcriptional activity. The tendency of yeast Hsf1 to phase separate may be linked to its extensive intrinsically disordered structure (**Figure 7A**), a feature proposed to be critical in the *in vivo* phase separation of other proteins (reviewed in (Alberti et al., 2019; Banani et al., 2017)). Given the link between Hsf1 condensation and transcription established in heat-shocked yeast cells, we anticipated that the appearance of Hsf1 condensates in ethanol-stressed cells would be delayed relative to the heat shock case, coinciding instead with the transcriptional induction of Hsf1-dependent genes. However, ethanol stress induced formation of Hsf1-GFP condensates as rapidly as heat shock. These were visible in virtually all cells as early as 2.5 min, paralleling the rapid appearance of Hsf1-GFP condensates in HS cells (**Figures 7C and 7D**; see **Figure 7B** for representative images). An independent analysis of Hsf1 tagged with a monomeric GFP derivative (mNeonGreen) gave virtually identical results; a large majority of cells exhibited Hsf1 puncta as early as 2.5 min exposure to 8.5% ethanol (**Figure 7 – figure supplement 1**). However, in contrast to the rapid dissolution of condensates in HS cells, those formed in ES cells appeared to be irreversible, as they showed no evidence of dissipating even after 150 min of continuous exposure to ethanol (**Figure 7 – figure supplement 1**). Indeed, Hsf1-GFP condensates were visible in cells exposed to 8.5% ethanol for at least 5.5 h (data not shown). Therefore, in ethanol-stressed cells, formation of Hsf1 condensates is uncoupled from *HSR* gene transcription and their maintenance is uncoupled from *HSR* gene repositioning. An important implication is that although condensates may initiate or promote *HSR* gene repositioning, they cannot maintain the 3D restructured state of the genome.

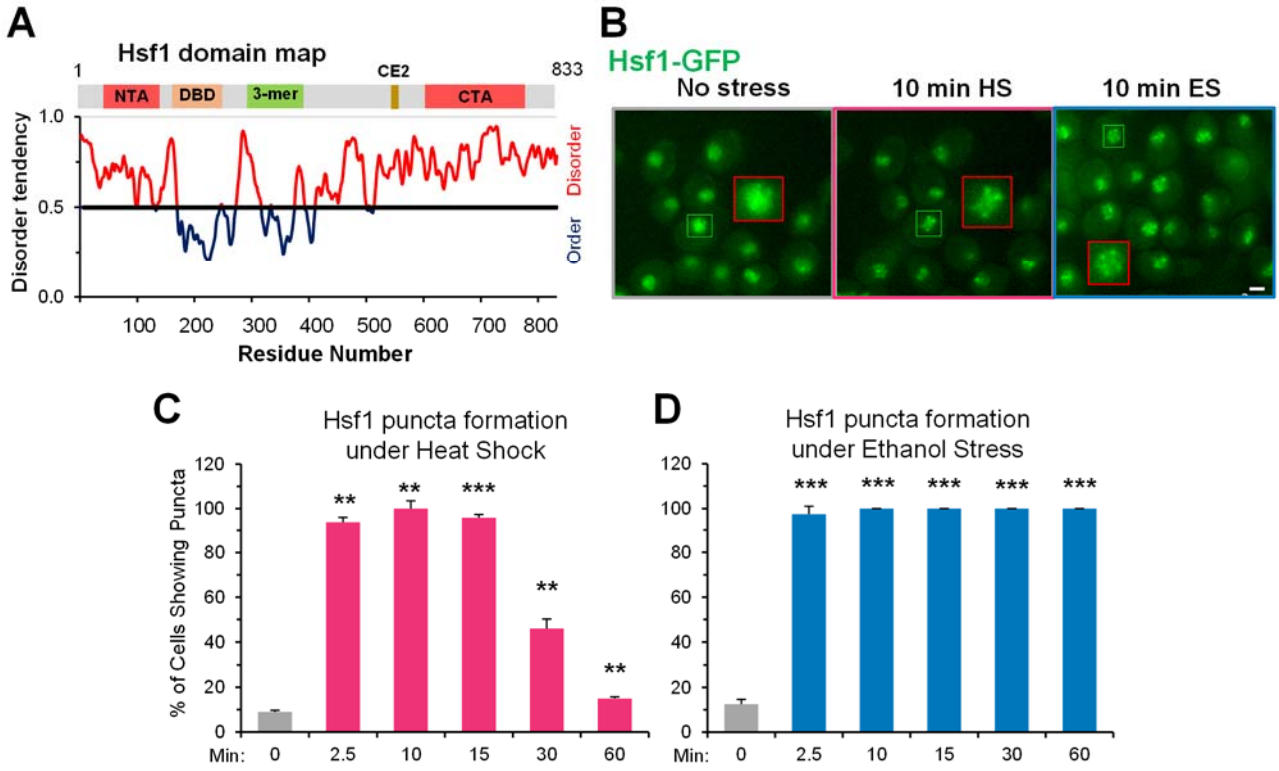

Figure 7. Ethanol stress induces rapid formation of long-lasting Hsf1 condensates

(A) Hsf1 is a transcription factor with high disorder tendency. The domain map for Hsf1 is shown at the top. Tendency for disorder was determined using IUPRED2.

(B) Condensate formation for Hsf1-GFP occurs in response to ethanol stress. Cells from the diploid strain ASK741 bearing Hsf1-GFP were grown in synthetic complete medium supplemented with adenine (SDC+Ade) and mounted onto ConA-coated coverslips (see Materials & Methods). Live cell widefield microscopy was performed for cells exposed to heat shock (HS, 38°C) or ethanol stress (ES, 8.5% v/v) or left untreated (25°C). A representative plane is shown for each condition out of 11 z-planes taken (interplanar distance of 0.5 µm). The red box indicates a zoomed image derived from the green boxed area. Scale bar: 2 µm.

(C) Cells from strain ASK741 were subjected to a 38°C heat shock for the indicated times and scored for the presence of Hsf1 condensates. A cell was deemed positive if it contained at least one clearly defined puncta. Approximately 200 cells were evaluated per field, per timepoint. A one-tailed t-test was used to assess significance of stress versus no stress condition. N=2. ***, p<0.01; ***, p<0.001.*

(D) Cells from strain ASK741 were exposed to 8.5% v/v ethanol for the indicated times and presence of Hsf1 condensates were scored from a total of 200 cells per field, per timepoint. Significance was determined as in (C).

Hsf1 and Pol II are required for *HSR* gene interactions in response to both heat shock and ethanol stress

The above analyses reveal several unexpected differences in the way yeast responds to ethanol stress versus heat stress: slow *HSR* gene transcriptional induction *versus* fast; delayed recruitment of RNA polymerase *versus* immediate; large initial increase in histone density *versus* minimal; sustained formation of Hsf1-containing condensates *versus* transient. Given these differences, we asked whether either Hsf1 or RNA Pol II are required for the repositioning of *HSR* genes in response to ethanol stress as both have been shown to be necessary for 3D genome restructuring in response to heat shock (Chowdhary et al., 2019, 2022). To do so, we used the auxin-induced degradation system to conditionally degrade either Hsf1 or the Rpb1 subunit of RNA Pol II in appropriately engineered strains. As schematically summarized in **Figure 8A**, cells expressing degron-tagged Hsf1 or Rpb1 were pre-treated with 1 mM IAA for 30-40 min, at which time each protein was >90% degraded (**Figure 8 – figure supplement 1A**). Loss of Rpb1 was associated with a growth defect detectable as early as 1 h, while its loss and that of Hsf1 were associated with loss of cell viability at all temperatures (**Figure 8 – figure supplement 1B, C**).

Strikingly, both intra- and inter-chromosomal interactions were nearly obviated in cells conditionally depleted of either Hsf1 or Rpb1 and then exposed to either stress (**Figure 8B, C)**. Close inspection of the data suggests that Hsf1 may make a more significant contribution, particularly in response to ethanol stress, since residual *HSR-HSR* gene interactions can be detected in Rpb1-depleted cells for certain pairwise tests. Together with the kinetic uncoupling of Pol II recruitment/transcription from *HSR* gene repositioning and the relative permanence of Hsf1 condensates under ES stress described above, these observations raise the possibility that ES-induced Hsf1 condensates are compositionally different from those formed in response to HS and drive *HSR* gene transcription in a mechanistically distinct way.

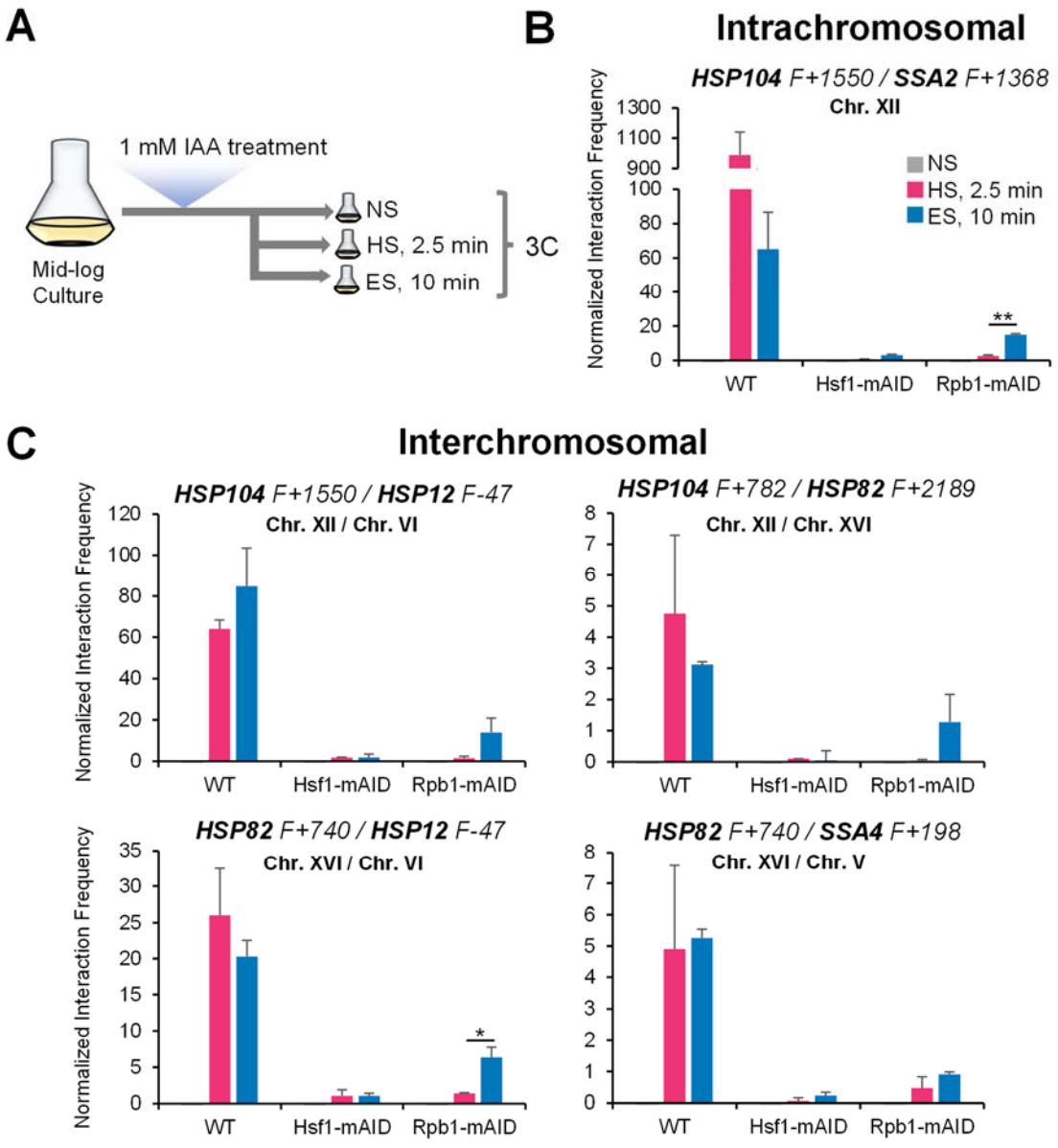

Figure 8. Hsf1 and Pol II are required for *HSR* gene interactions in response to both heat shock and ethanol stress

(A) Experimental strategy. Degron-tagged cells were treated with 1 mM indole acetic acid (IAA) at 25°C for 30-40 min prior to exposure to either heat shock (HS, 39°C for 2.5 min) or ethanol stress (ES, 8.5% v/v ethanol for 10 min) followed by HCHO crosslinking and 3C analysis. No Stress (NS) samples were maintained at 30°C for 10 min following IAA treatment and then crosslinked.

(B) Strains LRY016 (OsTIR1), LRY100 (OsTIR1, Hsf1-mAID) and LRY102 (OsTIR1, Rpb1-mAID) were subjected to the above protocol and physical interactions between the indicated chromosomal loci were detected by TaqI-3C (see Figure 4–figure supplement 1 for location of TaqI restriction sites). Shown is an example of intrachromosomal interactions. Graphs represent means + SD. One-tailed T-test. *, $p<0.05$.

(C) As in (B), but for interchromosomal interactions. One tailed-T-test. **, $p<0.01$.

Discussion

Ethanol stress induces *HSR* gene transcription, *HSR* gene coalescence and *HSR* condensate formation

Here we have shown that exposure of budding yeast to a high, but sub-lethal, concentration of ethanol strongly stimulates the binding of Hsf1 to the upstream regulatory regions of *HSR* genes. Unexpectedly, such binding – which is evident as early as 2.5 min – does not lead to concurrent recruitment of Pol II and transcription of *HSR* genes. Instead, Pol II recruitment and transcription are delayed, typically for 10 min or longer. As exposure to ethanol causes a global yet transient compaction of chromatin (discussed further below), the increase in nucleosome density may present a barrier to both Pol II recruitment and elongation. In addition, another feature of heat shocked-induced Hsf1 activation – repositioning of *HSR* genes within the 3D genome – is observed in cells exposed to ethanol. However, unlike transcription, this phenomenon occurs rapidly and is transient, resembling what is observed in heat shocked cells. The lack of temporal linkage between *HSR* gene transcription and *HSR* intergenic interactions is consistent with the idea that *HSR* gene coalescence and transcription are distinct phenomena and that Hsf1 can drive long-range changes in 3D genome structure independent of inducing transcription (with the best example being *HSP12* (**Figures 2B, 8C**)). These observations also demonstrate that a gene-specific TF can have functions independent of regulating transcription (discussed further below).

It has recently been demonstrated that in response to heat shock, inducible transcriptional condensates drive 3D genome reorganization in budding yeast. This conclusion arose from several features, including the tight temporal linkage between Hsf1 condensation and *HSR* intergenic interactions and the similar sensitivity of these two phenomena to the aliphatic alcohol, 1,6-hexanediol (Chowdhary et al., 2022). Consistent with previous observations of heat-shocked cells (and confirmed here), we have found that in response to ethanol stress, Hsf1 forms discrete puncta and that such puncta are detectable within 2.5 min. However, unlike the case with HS, Hsf1-containing condensates are stable – persisting for hours – while in HS cells such assemblies

dissipate within 30 min. In light of the transient nature of induced *HSR* intergenic interactions, we conclude that although condensates may initiate or promote *HSR* gene repositioning in ES cells, they cannot maintain the restructured genomic state. One possible explanation for the difference between ES- and HS-induced condensates is an altered composition of Hsf1 transcriptional condensates dependent on the stress. In heat-stressed cells, both Pol II and Mediator are efficiently incorporated into Hsf1-containing condensates (Chowdhary et al., 2022) while in ethanol-stressed cells neither Pol II and Mediator are incorporated (L.S. Rubio and D.S. Gross, manuscript in preparation**)**. Salient differences by which yeast cells respond to heat versus ethanol stress are summarized in Table 1.

Exposure to ethanol transiently induces global compaction of chromatin

An important observation is that exposure of cells to 8.5% ethanol leads to widespread compaction of chromatin. Although this effect is temporary, both euchromatic and heterochromatic regions are impacted as revealed by H3 ChIP, and this is consistent with measurements of total chromatin volume that reveal a decrease lasting nearly 60 min. A similar outcome was recently reported for both yeast and mammalian cells exposed to aliphatic di-alcohols (Itoh et al., 2021; Meduri et al., 2022). It is likely that the effect of ethanol exposure is nearly instantaneous since ethanol is known to denature proteins (Kato et al., 2019), likely by dehydration (disruption of biomolecules' hydration shell). While such denaturation may contribute to chromatin compaction, the effect is reversible, possibly due to refolding / renaturation mediated by Hsp70 and other molecular chaperones whose intracellular concentration increases during ethanol exposure. As mentioned above, the temporary effect on chromatin could suppress Pol II recruitment and subsequent elongation. Possible advantages of this chromatin compaction could be to downregulate global transcription, as well as to limit the chromatin damage by reactive oxygen species or other potentially damaging molecules present in the cell during stress conditions (Bradley et al., 2021; Costa et al., 1997; Davidson et al., 1996; Davidson & Schiestl, 2001; Shen et al., 2020; Voordeckers et al., 2020).

A novel function for a transcription factor that is uncoupled from regulating the transcription of its target gene

A key finding is that in response to ethanol stress, *HSR* genes reposition and Hsf1 condensates form well before transcription of Hsf1-dependent genes peaks, and in certain cases, is even detected. This suggests that Hsf1 has a functional role beyond regulating transcription since it forms nuclear condensates that drive the repositioning of *HSR* genes, culminating in their physical coalescence. A separation of function mutation in Hsf1 underscores this fact. Deletion of the N-terminal IDR / activation domain (amino acids 1-140; see Figure 7A) was observed to have little effect on *HSR* gene transcription during an acute heat shock yet intergenic 3C interactions were strongly suppressed (Chowdhary et al., 2022).

Conclusion

While Hsf1 is known to induce interactions between transcriptionally active *HSR* genes in response to heat shock, here we have demonstrated a similar role for this transcription factor in response to ethanol stress. Despite minimal *HSR* gene transcription during the initial 10 min exposure to ethanol, *HSR* genes engage in robust physical interactions, rivaling those seen for 2.5 min HS. This interaction correlates with an increase in definition of Hsf1 condensates yet is not accompanied by concurrent recruitment of Pol II to promoters, perhaps due to compaction of chromatin that occurs in ethanol-stressed cells. Hsf1 therefore forms condensates and drives 3D repositioning of its target genes without appreciably activating these genes. Furthermore, Hsf1 does this through formation of condensates that appear to be materially different than those that form in response to HS. Therefore, in ES cells, Hsf1 condensate formation and genome reorganization are not coupled with high transcriptional output, as is the case for HS (see **Figure 9** for model). Our results also argue that formation of TF clusters, while sufficient for TF DNA binding and 3D genome restructuring, is not sufficient to drive transcription. Additional factors and/or activities – such as the opening of chromatin – are necessary. Further research into the biophysical properties, molecular regulation, and functional consequences of HSF1 condensates will deepen our understanding of how cells respond to both thermal and chemical stress and maintain cellular homeostasis.

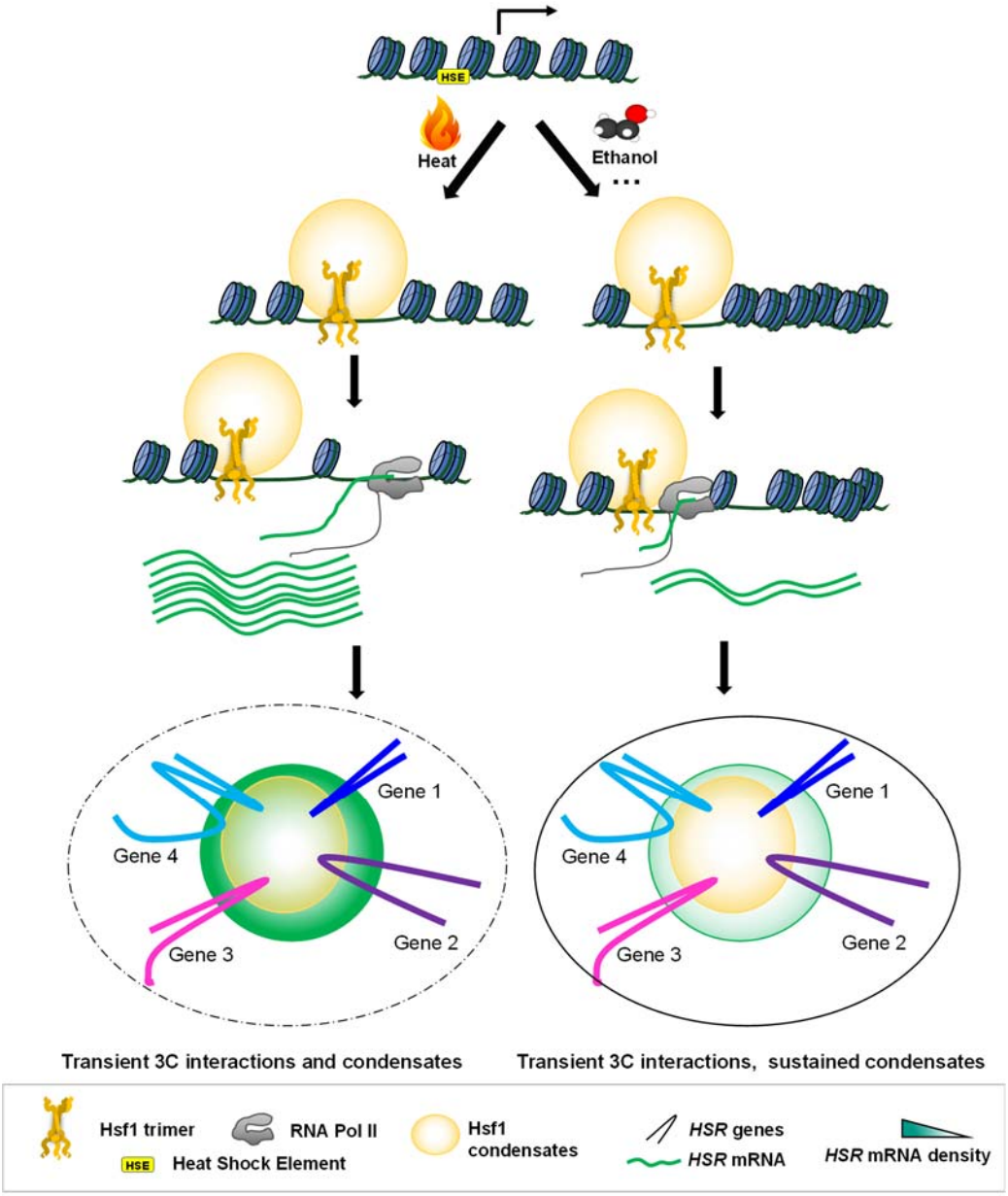

Figure 9. *Heat Shock Responsive* genes undergo rapid 3D genome repositioning following exposure to ethanol stress despite their delayed and muted transcription

Working model depicting the response of Hsf1-regulated genes in *Saccharomyces cerevisiae* under either heat shock (left) or ethanol stress (right).
Heat shock rapidly induces Hsf1 occupancy of Heat Shock Elements (HSEs) upstream of *HSR* genes, leading to fast and robust Pol II recruitment, histone eviction and high levels of *HSR* gene transcription. These parameters are kinetically linked to the coalescence of *HSR* genes and the presence of Hsf1 transcriptional condensates. Transcription at *HSR* genes decreases once the cell acclimates to the high temperature; this is accompanied by dissolution of condensates and relaxation of genome structure. All typically attenuate within 60 min.
Ethanol stress induces an initial chromatin compaction, which Hsf1 overcomes to bind HSEs, albeit with a slight delay (represented using ...). Hsf1 then recruits Pol II, but transcriptional output is markedly lower than under heat shock and this may be due to reduced productive elongation of Pol II through *HSR* coding regions. Despite the low transcriptional activity, *HSR* genes physically interact. Formation of Hsf1 condensates is kinetically linked to *HSR* intergenic interactions yet condensate presence is insufficient to maintain *HSR* interactions as the latter dissipate between 20 – 60 min. Hsf1 condensates persist for $\geq$2.5 h.

Materials and Methods

Yeast Strain Construction

The *HSF1-mNeonGreen* (*HSF1-mNG*) diploid strain LRY033 expressing a yeast-optimized version of mNeonGreen and co-expressing Sis1-mKate and Hsp104-BFP (mTagBFP2) was created as follows. First, DPY1561 (Feder et al., 2021) was crossed to W303-1B to create strain LRY031. This diploid was sporulated and a strain homozygous for *HSF1* and retention of one allele each of *SIS-mKate* and *HSP104-mTagBFP2* was obtained after back crossing. The resultant diploid was named LRY032. LRY032 was transformed with a PCR amplicon containing 50 bp of homology sequences flanking the stop codon, targeting the mNG tag to *HSF1* at its C-terminus flanked by the *HIS3* selectable marker. The plasmid template for this amplification was pFA6a-link-ymNeonGreen-SpHis5 (Botman et al., 2019). LRY033 is heterozygous for *HSF1-mNG, SIS1-mKate* and *HSP104-mTagBFP2.*

Other strains were created as follows. LRY037 was constructed using the *HSF1*-targeted *mNeonGreen* amplicon to transform strain W303-1B. LRY040 was constructed by transforming LRY037 with an amplicon containing *RPB3-mCherry::hphMX6*, obtained using genomic DNA from strain SCY004 (Chowdhary et al., 2022) as template. LRY100 and LRY102 were constructed using LRY016 (Rubio & Gross, 2023) as recipient of the mini-degron tag amplified from pHyg-AID*-9myc (Morawska & Ulrich, 2013), targeted to the C-terminus of *HSF1* and *RPB1*, respectively.

A complete list of strains as well as plasmids and primers used in strain construction are listed in **Supplemental File 1 – Tables 1, 2, 3**.

Yeast culture and treatment conditions

Cells were grown at 30°C in YPDA (1% w/v yeast extract, 2% w/v peptone, 2% w/v dextrose and 20 mg/L adenine) to mid-log density (OD_{600}= 0.6 – 0.8). For ethanol stress, the cell culture was mixed with an equal volume of YPDA containing 17% v/v ethanol (yielding a final concentration of 8.5%) and incubated at 25°C for different

lengths of time as indicated in the figures. For heat shock, the mid-log culture was mixed with an equal volume of 55°C YPDA medium to achieve an instantaneous temperature upshift to 39°C, and the culture was maintained at 39°C for the indicated times. The no stress samples were diluted with an equivalent volume of YPDA and maintained at 25°C. Samples were kept at their respective temperatures using a water bath with constant shaking.

Cell Viability and Growth Assays

Cell Viability Assay

Cells were grown at 30°C in YPDA to OD_{600}=0.6 and then diluted to OD_{600}=0.4 using an equivalent volume of medium as described above for ethanol stress, heat shock or the no stress control (YPDA at 25°C). Cells were kept under these conditions for 3 h; during this time aliquots were taken at different timepoints and diluted 1:26,000 for plating onto YPDA. Plates were incubated at 30°C for 3 days then scanned. Colonies were quantified using ImageJ/Fiji (v. 1.53t) (Schindelin et al., 2012) - “Analyze Particles” option. The number of colony-forming units (CFUs) obtained in stress samples were normalized to the no stress samples and expressed as a percentage of the number of CFUs obtained in the no stress sample.

Growth Assay

Cells were grown in liquid culture and subjected to the same treatments as described above. OD_{600} readings of each sample were taken at intervals over 3 h (see Figure 1). The average OD_{600} from two samples was plotted versus time.

Auxin Induced Degradation

Cells expressing the F-box protein osTIR1 in combination with a degron-tagged protein were grown in YPDA medium to mid-log phase and indole-3-acetic acid (IAA) was then added to a final concentration of 1 mM. IAA stocks [10 mg/mL (57 mM)] were prepared fresh in 95% ethanol and filter-sterilized before use. For immunoblot analysis, cells were treated for varying times up to 1 h prior to metabolic arrest using 20 mM sodium azide, followed by cell harvesting. 0 min control samples were treated with vehicle alone (1.7% v/v ethanol). For growth curve analysis, samples were kept at 30°C with constant shaking and aliquots were removed at various timepoints to monitor OD_{600}. For 3C

analysis, cells were similarly grown in YPDA to OD_{600}=0.6, then treated with 1 mM IAA for either 30 min (LRY016 and LRY100) or 40 min (LRY102) prior to cell cross-linking and subsequent cell harvesting.

Reverse transcription-quantitative PCR (RT-qPCR)

RT-qPCR was conducted as previously described using 25 mL cell culture aliquots (Rubio & Gross, 2023). PCR primers used are listed in **Supplemental File 1 – Table 4**.

Chromatin Immunoprecipitation

Chromatin immunoprecipitation was performed as previously described (Chowdhary et al 2019) with modifications. Briefly, cells from a 50 mL mid-log culture were exposed to 8.5% v/v ethanol and fixed using 3.01% formaldehyde (HCHO), resulting in a net concentration of 1%. Glycine was then added to 0.363 M glycine to quench excess formaldehyde. (Note: HCHO is consumed in a reaction with ethanol. Since 8.5% ethanol equals 1.46 M, acetal formation at 1:2 stoichiometry consumes 0.730 M (2.01%) of HCHO, leaving an effective concentration of 0.363 M (1%). The reaction resulting in formation of an acetal is illustrated in **Figure 10**.

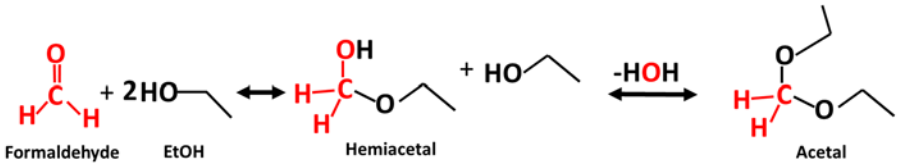

Figure 10. Acetal formation reaction (McMurry, 2012)

For heat shock, cells from a 50 mL mid-log culture were fixed with 1% formaldehyde following 39°C upshift for the times indicated (Figure 3). Glycine was then added at a final concentration of 0.363 M to quench unreacted formaldehyde. Chromatin lysates, prepared as previously described (Chowdhary et al., 2019), were incubated using 20% of the lysate with one of the following antibodies: 1.5 µL of anti-Hsf1 (Erkine et al., 1996), 1.5 µL anti-Rpb1 antiserum (Zhao et al., 2005), or 1 µL of H3 antibody (Abcam, ab1791). Incubation of lysate with antibody was done for 16 h at 4°C. Chromatin fragments bound to antibody were captured on Protein A-Sepharose beads (GE

Healthcare) for 16 h at 4°C. Wash, elution, and DNA purification were conducted as described (Chowdhary et al., 2019). The ChIP DNA template was quantified by qPCR (7900HT Fast Real Time PCR System, Applied Biosystems). A standard curve was generated using genomic DNA and ChIP DNA quantities were deduced by interpolation. The qPCR signal for each primer combination was normalized relative to the corresponding signal arising from the input DNA. Primers used in ChIP analysis are listed in **Supplemental File 1 – Table 5**.

Taq I chromosome conformation capture (Taq I-3C)

TaqI-3C was performed as previously described (Rubio & Gross, 2023). A master cell culture was grown at 30°C in YPDA from OD_{600}=0.15 to a final OD_{600}=0.8. Aliquots of 50 mL were used for each condition. Heat shock and ethanol stress were conducted as described above. Primers for analysis of 3C templates are listed in **Supplemental File 1 – Table 6**.

Fluorescence Microscopy

Widefield Fluorescence Microscopy

For Figures 6B, 6C and 7, cells were grown at 30°C in Synthetic Complete Dextrose (SDC) medium supplemented with 0.1 mg/mL adenine to early log phase. From this culture, 90 µL were removed and cells were immobilized onto a concanavalin A (ConA, Sigma Aldrich, 100 µg/mL in ddH_2O)-coated coverslip for 20 min. The medium was then removed and replaced by either SDC or SDC + 8.5% v/v ethanol. The coverslip was mounted onto a concave microscope slide (2-Well Concavity Slide, Electron Microscopy Sciences). Images were acquired using an AX70 Olympus epifluorescence microscope across 11 z-planes with 0.5 µm of interplanar distance. Filter set 89021 (Chroma Technology) and a Photometrics Prime 95B camera were used to image GFP and mCherry. SlideBook Software version 6.0.15 (Intelligent Imaging Innovations) was used for image capturing and z-axis stepping motor operation (Ludl Electronic products).

For heat shock, No Stress (NS) control images were taken using an Olympus Ach 100/1.25-NA objective coupled to a heating device (Bioptechs objective heater system).

Heat-shocked sample imaging was done by rotating the objective away from the coverslip, switching the heating system on, and allowing it to reach 38°C before returning the objective to the coverslip for an instantaneous heat shock. The same field of view on the coverslip was imaged for both NS and HS timepoints. For ethanol stress, an Olympus UPlanFl 100/1.4-NA objective was used for image acquisition. Analysis of the images after acquisition was done using ImageJ (v. 1.52).

In the *HSP104-TMA10* coalescence analysis, cells in which the fluorophore-tagged genes had undergone replication (two green or two red fluorescent spots, indicative of late S/G2 phase) were excluded from the analysis. The locations of the two tagged loci were analyzed over 11 different z-planes, encompassing the whole nucleus. Cells were deemed coalescence positive if they displayed colocalized, non-resolvable fluorophore signals with a distance of <0.4 µm between centroids.

Spinning Disk Confocal Microscopy

For all other imaging figures, cells were grown as described above and image acquisition was done using an UPlan Apo 100x/1.50 NA objective in an Olympus Yokogawa CSU W1 Spinning Disk Confocal System coupled to sCMOS cameras (Hamamatsu Fusion) controlled by CellSens Dimension software. A 50µm pinhole disk was used for imaging in combination with 10% of laser power employed for excitation using 405 nm, 488 nm, and 561 nm lasers. Z-stacks were captured as for widefield fluorescence. For heat shock, cells were attached to a VAHEAT substrate (Icha et al., 2022) using ConA as above. The substrate was mounted onto the VAHEAT holder and control images were captured before heat was applied. Samples were instantaneously heated to 39°C. The substrate reservoir was covered with a coverslip to prevent media evaporation. Imaging was done over multiple timepoints as indicated in the figures. For ethanol stress, cells were mounted onto a coverslip as above, petroleum jelly was used to hold the coverslip against the concave slide. The slide was inverted and placed on the stage for visualization at room temperature.

Image reconstruction and analysis was done using FIJI/ImageJ (v. 1.53t) (Schindelin et al., 2012). Hsp104-BFP (LRY033) and Hsf1-mNeonGreen (LRY040) foci count were performed using the “Cells” feature in Imaris v.10.0.0. For analysis of transcription in VPY705, *MS2x24-HSP104* mRNA was visualized using the signal arising from MCP-mCherry binding to the chimeric transcript. Cells were interrogated for transcription by assaying the presence of an mCherry focus adjacent to *HSP104-LacO*$_{256}$ bound by LacI-GFP. The high background signal from MCP-mCherry made it difficult to assess the localization of transcripts once they dissociated from the *HSP104*-tagged gene.

Acknowledgments

We thank Drs. Kelly Tatchell, Lucy C. Robinson, Rini Ravindran, Eric First, Surabhi Chowdhary and David Pincus for helpful discussions and technical advice; Drs. Vickky Pandit and Amoldeep Kainth for strain construction; Paula Polk for help with quantitative PCR; and Drs. Donna and Jason Brickner, Surabhi Chowdhary, Amoldeep Kainth and David Pincus for generously providing yeast strains. This work was supported by NIH grants R01 GM138988 and R15 GM128065 awarded to D.S.G. and an Ike Muslow predoctoral fellowship awarded to L.S.R.

Author Contributions

Linda S. Rubio, Conceptualization, Investigation, Visualization, Methodology, Formal Analysis, Writing – original draft, Writing – review and editing; Suman Mohajan, Investigation, Visualization, Methodology, Formal Analysis; David S. Gross, Conceptualization, Resources, Visualization, Validation, Supervision, Funding Acquisition, Writing – original draft, Writing – review and editing.

References

Albert, B., Kos-Braun, I. C., Henras, A. K., Dez, C., Rueda, M. P., Zhang, X., Gadal, O., Kos, M., & Shore, D. (2019). A ribosome assembly stress response regulates transcription to maintain proteome homeostasis. *ELife*, *8*. https://doi.org/10.7554/eLife.45002

Alberti, S., Gladfelter, A., & Mittag, T. (2019). Considerations and Challenges in Studying Liquid-Liquid Phase Separation and Biomolecular Condensates. *Cell*, *176*(3), 419–434. https://doi.org/10.1016/j.cell.2018.12.035

Ali, A., Garde, R., Schaffer, O. C., Bard, J. A. M., Husain, K., Kik, S. K., Davis, K. A., Luengo-Woods, S., Drummond, D. A., Squires, A. H., & Pincus, D. (2022). Adaptive preservation of orphan ribosomal proteins in chaperone-stirred condensates. *BioRxiv*, 2022.11.09.515856. doi: https://doi.org/10.1101/2022.11.09.515856

Ansari, A., & Hampsey, M. (2005). A role for the CPF 3′ -end processing machinery in RNAP II-dependent gene looping. *Genes and Development*, *19*(24), 2969–2978. https://doi.org/10.1101/gad.1362305

Banani, S. F., Lee, H. O., Hyman, A. A., & Rosen, M. K. (2017). Biomolecular condensates: Organizers of cellular biochemistry. *Nature Reviews Molecular Cell Biology*, *18*(5), 285–298. https://doi.org/10.1038/nrm.2017.7

Bandas, E. L., & Zakharov, I. A. (1980). Induction of rho- mutations in yeast Saccharomyces cerevisiae by ethanol. *Mutation Research*, *71*(2), 193–199. https://doi.org/10.1016/0027-5107(80)90070-6

Boija, A., Klein, I. A., Sabari, B. R., Dall'Agnese, A., Coffey, E. L., Zamudio, A. V., Li, C. H., Shrinivas, K., Manteiga, J. C., Hannett, N. M., Abraham, B. J., Afeyan, L. K., Guo, Y. E., Rimel, J. K., Fant, C. B., Schuijers, J., Lee, T. I., Taatjes, D. J., & Young, R. A. (2018). Transcription Factors Activate Genes through the Phase-Separation Capacity of Their Activation Domains. *Cell*, *175*(7), 1842-1855.e16. https://doi.org/10.1016/j.cell.2018.10.042

Botman, D., de Groot, D. H., Schmidt, P., Goedhart, J., & Teusink, B. (2019). In vivo characterisation of fluorescent proteins in budding yeast. *Scientific Reports*, *9*(1). https://doi.org/10.1038/s41598-019-38913-z

Bradley, A. I., Marsh, N. M., Borror, H. R., Mostoller, K. E., Gama, A. I., & Gardner, R. G. (2021). Acute ethanol stress induces sumoylation of conserved chromatin structural proteins in Saccharomyces cerevisiae. *Molecular Biology of the Cell*, *32*, 1121–1133. https://doi.org/10.1091/mbc.e20-11-0715

Bresson, S., Shchepachev, V., Spanos, C., Turowski, T. W., Rappsilber, J., & Tollervey, D. (2020). Stress-Induced Translation Inhibition through Rapid Displacement of Scanning Initiation Factors. *Molecular Cell*, *80*(0). https://doi.org/10.1016/j.molcel.2020.09.021

Brickner, D. G., Randise-Hinchliff, C., Corbin, M. L., Liang, J. M., Kim, S., Sump, B., D'Urso, A., Kim, S. H., Satomura, A., Schmit, H., Coukos, R., Hwang, S., Watson, R., & Brickner, J. H. (2019). The Role of Transcription Factors and Nuclear Pore Proteins in Controlling the Spatial Organization of the Yeast Genome. *Developmental Cell*, *49*(6), 936-947.e4. https://doi.org/10.1016/j.devcel.2019.05.023

Brickner, J. H., & Walter, P. (2004). Gene recruitment of the activated INO1 locus to the nuclear membrane. *PLoS Biology*, *2*(11), e342. https://doi.org/10.1371/journal.pbio.0020342

Cabal, G. G., Genovesio, A., Rodriguez-Navarro, S., Zimmer, C., Gadal, O., Lesne, A., Buc, H., Feuerbach-Fournier, F., Olivo-Marin, J. C., Hurt, E. C., & Nehrbass, U. (2006). SAGA interacting factors confine sub-diffusion of transcribed genes to the nuclear envelope. *Nature*, *441*(7094), 770–773. https://doi.org/10.1038/nature04752

Casolari, J. M., Brown, C. R., Komili, S., West, J., Hieronymus, H., & Silver, P. A. (2004). Genome-wide localization of the nuclear transport machinery couples transcriptional status and nuclear organization. *Cell*, *117*(4), 427–439. https://doi.org/10.1016/S0092-8674(04)00448-9

Cho, W. K., Spille, J. H., Hecht, M., Lee, C., Li, C., Grube, V., & Cisse, I. I. (2018). Mediator and RNA polymerase II clusters associate in transcription-dependent condensates. *Science*, *361*(6400), 412–415. https://doi.org/10.1126/science.aar4199

Chowdhary, S., Kainth, A. S., & Gross, D. S. (2017). Heat Shock Protein Genes Undergo Dynamic Alteration in Their Three-Dimensional Structure and Genome Organization in Response to Thermal Stress. *Molecular and Cellular Biology*, *37*(24), 1–23. https://doi.org/10.1128/mcb.00292-17

Chowdhary, S., Kainth, A. S., & Gross, D. S. (2020). Chromosome conformation capture that detects novel cis- and trans-interactions in budding yeast. *Methods*, *170*, 4–16. https://doi.org/10.1016/j.ymeth.2019.06.023

Chowdhary, S., Kainth, A. S., Paracha, S., Gross, D. S., & Pincus, D. (2022). Inducible transcriptional condensates drive 3D genome reorganization in the heat shock response. *Molecular Cell*, *82*(22), 4386-4399.e7. https://doi.org/10.1016/j.molcel.2022.10.013

Chowdhary, S., Kainth, A. S., Pincus, D., & Gross, D. S. (2019). Heat Shock Factor 1 Drives Intergenic Association of Its Target Gene Loci upon Heat Shock. *Cell Reports*, *26*(1), 18-28.e5. https://doi.org/10.1016/j.celrep.2018.12.034

Costa, V., Amorim, M. A., Reis, E., Quintanilha, A., & Moradas-Ferreira, P. (1997). Mitochondrial superoxide dismutase is essential for ethanol tolerance of Saccharomyces cerevisiae in the post-diauxic phase. *Microbiology*, *143*(5), 1649–1656. https://doi.org/10.1099/00221287-143-5-1649

Davidson, J. F., & Schiestl, R. H. (2001). Mitochondrial Respiratory Electron Carriers Are Involved in Oxidative Stress during Heat Stress in Saccharomyces cerevisiae . *Molecular and Cellular Biology*, *21*(24), 8483–8489. https://doi.org/10.1128/mcb.21.24.8483-8489.2001

Davidson, J. F., Whyte, B., Bissinger, P. H., & Schiestl, R. H. (1996). Oxidative stress is involved in heat-induced cell death in Saccharomyces cerevisiae. *Proceedings of the National Academy of Sciences of the United States of America*, *93*(10), 5116–5121. https://doi.org/10.1073/pnas.93.10.5116

Dieppois, G., Iglesias, N., & Stutz, F. (2006). Cotranscriptional Recruitment to the mRNA Export Receptor Mex67p Contributes to Nuclear Pore Anchoring of Activated Genes. *Molecular and Cellular Biology*, *26*(21), 7858–7870. https://doi.org/10.1128/mcb.00870-06

Duan, Z., Andronescu, M., Schutz, K., McIlwain, S., Kim, Y. J., Lee, C., Shendure, J., Fields, S., Blau, C. A., & Noble, W. S. (2010). A three-dimensional model of the yeast genome. *Nature*, *465*(7296), 363–367. https://doi.org/10.1038/nature08973

Erkine, A. M., Adams, C. C., Diken, T., & Gross, D. S. (1996). Heat shock factor gains access to the yeast HSC82 promoter independently of other sequence-specific factors and antagonizes nucleosomal repression of basal and induced transcription. *Molecular and Cellular Biology*, *16*(12), 7004–7017.

Eser, U., Chandler-Brown, D., Ay, F., Straight, A. F., Duan, Z., Noble, W. S., & Skotheim, J. M. (2017). Form and function of topologically associating genomic domains in budding yeast. *Proceedings of the National Academy of Sciences of the United States of America*, *114*(15), E3061–E3070. https://doi.org/10.1073/pnas.1612256114

Fanucchi, S., Shibayama, Y., Burd, S., Weinberg, M. S., & Mhlanga, M. M. (2013). Chromosomal contact permits transcription between coregulated genes. *Cell*, *155*(3), 606. https://doi.org/10.1016/J.CELL.2013.09.051

Feder, Z. A., Ali, A., Singh, A., Krakowiak, J., Zheng, X., Bindokas, V. P., Wolfgeher, D., Kron, S. J., & Pincus, D. (2021). Subcellular localization of the J-protein Sis1 regulates the heat shock response. *Journal of Cell Biology*, *220*(1), e202005165. https://doi.org/10.1083/JCB.202005165

Gasch, A. P., Spellman, P. T., Kao, C. M., Carmel-Harel, O., Eisen, M. B., Storz, G., Botstein, D., & Brown, P. O. (2000). Genomic expression programs in the response of yeast cells to environmental changes. *Molecular Biology of the Cell*, *11*(12), 4241–4257. https://doi.org/10.1091/mbc.11.12.4241

Green, E. M., Jiang, Y., Joyner, R., & Weis, K. (2012). A negative feedback loop at the nuclear periphery regulates GAL gene expression. *Molecular Biology of the Cell*, *23*(7), 1367–1375. https://doi.org/10.1091/mbc.E11-06-0547

Grouši, T., Ivanov, P., Frýdlová, I., Vašicová, P., Janda, F., Vojtová, J., Malínská, K., Malcová, I., Nováková, L., Janošková, D., Valášek, L., & Hašek, J. (2009). Robust heat shock induces eIF2α-phosphorylationin-dependent assembly of stress granules containing eIF3 and 40S ribosomal subunits in budding yeast, Saccharomyces cerevisiae. *Journal of Cell Science*, *122*(12), 2078–2088. https://doi.org/10.1242/jcs.045104

Haim, L., Zipor, G., Aronov, S., & Gerst, J. E. (2007). A genomic integration method to visualize localization of endogenous mRNAs in living yeast. *Nature Methods*, *4*(5), 409–412. https://doi.org/10.1038/nmeth1040

Hnisz, D., Shrinivas, K., Young, R. A., Chakraborty, A. K., & Sharp, P. A. (2017). A Phase Separation Model for Transcriptional Control. *Cell*, *169*(1), 13–23. https://doi.org/10.1016/j.cell.2017.02.007

Homoto, S., & Izawa, S. (2018). Persistent actin depolarization caused by ethanol induces the formation of multiple small cortical septin rings in yeast. *Journal of Cell Science*, *131*(15). https://doi.org/10.1242/jcs.217091

Hsieh, T. H. S., Weiner, A., Lajoie, B., Dekker, J., Friedman, N., & Rando, O. J. (2015). Mapping Nucleosome Resolution Chromosome Folding in Yeast by Micro-C. *Cell*, *162*(1), 108–119. https://doi.org/10.1016/j.cell.2015.05.048

Icha, J., Böning, D., & Türschmann, P. (2022). Precise and Dynamic Temperature Control in High-Resolution Microscopy with VAHEAT. *Microscopy Today*, *30*(1),

34–41. https://doi.org/10.1017/s1551929521001553
Itoh, Y., Iida, S., Tamura, S., Nagashima, R., Shiraki, K., Goto, T., Hibino, K., Ide, S., & Maeshima, K. (2021). 1,6-hexanediol rapidly immobilizes and condenses chromatin in living human cells. *Life Science Alliance*, *4*(4). https://doi.org/10.26508/LSA.202001005
Johnston, G. C., & Singer, R. A. (1980). Ribosomal precursor RNA metabolism and cell division in the yeast Saccharomyces cerevisiae. *Molecular & General Genetics*, *178*(2), 357–360. https://doi.org/10.1007/BF00270484
Kato, K., Yamamoto, Y., & Izawa, S. (2011). Severe ethanol stress induces assembly of stress granules in Saccharomyces cerevisiae. *Yeast*, *28*(5), 339–347. https://doi.org/10.1002/yea.1842
Kato, S., Yoshida, M., & Izawa, S. (2019). Btn2 is involved in the clearance of denatured proteins caused by severe ethanol stress in Saccharomyces cerevisiae. *FEMS Yeast Research*, *19*(8), 1–8. https://doi.org/10.1093/femsyr/foz079
Kim, S., & Gross, D. S. (2013). Mediator recruitment to heat shock genes requires dual Hsf1 activation domains and Mediator tail subunits Med15 and Med16. *Journal of Biological Chemistry*, *288*(17), 12197–12213. https://doi.org/10.1074/jbc.M112.449553
Krakowiak, J., Zheng, X., Patel, N., Feder, Z. A., Anandhakumar, J., Valerius, K., Gross, D. S., Khalil, A. S., & Pincus, D. (2018). Hsf1 and Hsp70 constitute a two-component feedback loop that regulates the yeast heat shock response. *ELife*, *7*, 1–17. https://doi.org/10.7554/eLife.31668
Kremer, S. B., & Gross, D. S. (2009). SAGA and Rpd3 chromatin modification complexes dynamically regulate heat shock gene structure and expression. *Journal of Biological Chemistry*, *284*(47), 32914–32931.
Kubota, S., Takeo, I., Kume, K., Kanai, M., Shitamukai, A., Mizunuma, M., Miyakawa, T., Shimoi, H., Iefuji, H., & Hirata, D. (2004). Effect of ethanol on cell growth of budding yeast: Genes that are important for cell growth in the presence of ethanol. *Bioscience, Biotechnology and Biochemistry*, *68*(4), 968–972. https://doi.org/10.1271/bbb.68.968
Lee, M. S., & Garrard, W. T. (1991). Transcription-induced nucleosome “splitting”: An underlying structure for DNase I sensitive chromatin. *EMBO Journal*, *10*(3), 607–615. https://doi.org/10.1002/j.1460-2075.1991.tb07988.x
Liti, G. (2015). The fascinating and secret wild life of the budding yeast S. cerevisiae. *ELife*, *4*. https://doi.org/10.7554/eLife.05835
Liu, B., Larsson, L., Caballero, A., Hao, X., Öling, D., Grantham, J., & Nyström, T. (2010). The Polarisome Is Required for Segregation and Retrograde Transport of Protein Aggregates. *Cell*, *140*(2), 257–267. https://doi.org/10.1016/j.cell.2009.12.031
McMurry, J. (2012). *Organic Chemistry* (L. Lockwood, S. Kiselica, & E. Woods (eds.); 8th ed.). Brooks/Cole.
Meduri, R., Rubio, L. S., Mohajan, S., & Gross, D. S. (2022). Phase-separation antagonists potently inhibit transcription and broadly increase nucleosome density. *Journal of Biological Chemistry*, *298*(10), 102365. https://doi.org/10.1016/j.jbc.2022.102365
Monahan, K., & Lomvardas, S. (2015). Monoallelic Expression of Olfactory Receptors.

Annual Review of Cell and Developmental Biology, *31*, 721–740. https://doi.org/10.1146/annurev-cellbio-100814-125308

Morawska, M., & Ulrich, H. D. (2013). An expanded tool kit for the auxin-inducible degron system in budding yeast. *Yeast*, *30*(9), 341–351. https://doi.org/10.1002/yea.2967

Nair, S. J., Yang, L., Meluzzi, D., Oh, S., Yang, F., Friedman, M. J., Wang, S., Suter, T., Alshareedah, I., Gamliel, A., Ma, Q., Zhang, J., Hu, Y., Tan, Y., Ohgi, K. A., Jayani, R. S., Banerjee, P. R., Aggarwal, A. K., & Rosenfeld, M. G. (2019). Phase separation of ligand-activated enhancers licenses cooperative chromosomal enhancer assembly. *Nature Structural and Molecular Biology*, *26*(3), 193–203. https://doi.org/10.1038/s41594-019-0190-5

O'Sullivan, J. M., Tan-Wong, S. M., Morillon, A., Lee, B., Coles, J., Mellor, J., & Proudfoot, N. J. (2004). Gene loops juxtapose promoters and terminators in yeast. *Nature Genetics*, *36*(9), 1014–1018.

Papantonis, A., Kohro, T., Baboo, S., Larkin, J. D., Deng, B., Short, P., Tsutsumi, S., Taylor, S., Kanki, Y., Kobayashi, M., Li, G., Poh, H. M., Ruan, X., Aburatani, H., Ruan, Y., Kodama, T., Wada, Y., & Cook, P. R. (2012). TNFα signals through specialized factories where responsive coding and miRNA genes are transcribed. *EMBO Journal*, *31*(23), 4404–4414. https://doi.org/10.1038/emboj.2012.288

Park, S. K., Xiang, Y., Feng, X., & Garrard, W. T. (2014). Pronounced cohabitation of active immunoglobulin genes from three different chromosomes in transcription factories during maximal antibody synthesis. *Genes and Development*, *28*(11), 1159–1164. https://doi.org/10.1101/gad.237479.114

Peffer, S., Gonçalves, D., & Morano, K. A. (2019). Regulation of the Hsf1-dependent transcriptome via conserved bipartite contacts with Hsp70 promotes survival in yeast. *Journal of Biological Chemistry*, *294*(32), 12191–12202.

Pincus, D., Anandhakumar, J., Thiru, P., Guertin, M. J., Erkine, A. M., & Gross, D. S. (2018). Genetic and epigenetic determinants establish a continuum of Hsf1 occupancy and activity across the yeast genome. *Molecular Biology of the Cell*, *29*(26), 3168–3182. https://doi.org/10.1091/mbc.E18-06-0353

Piper, P. W. (1995). The heat shock and ethanol stress responses of yeast exhibit extensive similarity and functional overlap. *FEMS Microbiology Letters*, *134*(2–3), 121–127. doi:10.1111/j.1574-6968.1995.tb07925.x

Piper, P. W., Talreja, K., Panaretou, B., Moradas-Ferreira, P., Byrne, K., Praekelt, U. M., Meacock, P., Recnacq, M., & Boucherie, H. (1994). Induction of major heat-shock proteins of Saccharomyces cerevisiae, including plasma membrane Hsp30, by ethanol levels above a critical threshold. *Microbiology*, *140*(11), 3031–3038. https://doi.org/10.1099/13500872-140-11-3031

Piškur, J., Rozpedowska, E., Polakova, S., Merico, A., & Compagno, C. (2006). How did Saccharomyces evolve to become a good brewer? *Trends in Genetics*, *22*(4), 183–186. https://doi.org/10.1016/j.tig.2006.02.002

Plesset, J., Palm, C., & McLaughlin, C. S. (1982). Induction of heat shock proteins and thermotolerance by ethanol in Saccharomyces cerevisiae. *Biochemical and Biophysical Research Communications*, *108*(3), 1340–1345. https://doi.org/10.1016/0006-291X(82)92147-7

Rosa, M. F., & Sá-Correia, I. (1991). In vivo activation by ethanol of plasma membrane

ATPase of Saccharomyces cerevisiae. *Applied and Environmental Microbiology*, *57*(3), 830–835. https://doi.org/10.1128/aem.57.3.830-835.1991

Rosa, M. F., & Sá-Correia, I. (1996). Intracellular acidification does not account for inhibition of Saccharomyces cerevisiae growth in the presence of ethanol. *FEMS Microbiology Letters*, *135*(2–3), 271–274. doi: 10.1111/j.1574-6968.1996.tb08000.x

Rozpedowska, E., Hellborg, L., Ishchuk, O. P., Orhan, F., Galafassi, S., Merico, A., Woolfit, M., Compagno, C., & Piškur, J. (2011). Parallel evolution of the make-accumulate-consume strategy in Saccharomyces and Dekkera yeasts. *Nature Communications*, *2*(1), 1–7. https://doi.org/10.1038/ncomms1305

Rubio, L. S., & Gross, D. S. (2023). Dynamic coalescence of yeast Heat Shock Protein genes bypasses the requirement for actin. *Genetics*. https://doi.org/10.1093/genetics/iyad006

Sabari, B. R., Dall'Agnese, A., Boija, A., Klein, I. A., Coffey, E. L., Shrinivas, K., Abraham, B. J., Hannett, N. M., Zamudio, A. V., Manteiga, J. C., Li, C. H., Guo, Y. E., Day, D. S., Schuijers, J., Vasile, E., Malik, S., Hnisz, D., Lee, T. I., Cisse, I. I., … Young, R. A. (2018). Coactivator condensation at super-enhancers links phase separation and gene control. *Science*, *361*(6400), eaar3958. https://doi.org/10.1126/science.aap9195

Schindelin, J., Arganda-Carreras, I., Frise, E., Kaynig, V., Longair, M., Pietzsch, T., Preibisch, S., Rueden, C., Saalfeld, S., Schmid, B., Tinevez, J. Y., White, D. J., Hartenstein, V., Eliceiri, K., Tomancak, P., & Cardona, A. (2012). Fiji: An open-source platform for biological-image analysis. *Nature Methods*, *9*(7), 676–682. https://doi.org/10.1038/nmeth.2019

Schoenfelder, S., Sexton, T., Chakalova, L., Cope, N. F., Horton, A., Andrews, S., Kurukuti, S., Mitchell, J. A., Umlauf, D., Dimitrova, D. S., Eskiw, C. H., Luo, Y., Wei, C. L., Ruan, Y., Bieker, J. J., & Fraser, P. (2010). Preferential associations between co-regulated genes reveal a transcriptional interactome in erythroid cells. *Nature Genetics*, *42*(1), 53–61. https://doi.org/10.1038/ng.496

Schulz, K. N., & Harrison, M. M. (2019). Mechanisms regulating zygotic genome activation. *Nature Reviews Genetics*, *20*(4), 221–234. https://doi.org/10.1038/s41576-018-0087-x

Sekinger, E. A., & Gross, D. S. (2001). Silenced chromatin is permissive to activator binding and PIC recruitment. *Cell*, *105*(3), 403–414.

Shen, L., Wang, Y. T., Tang, X. X., Zhang, K., Wang, P. M., Sui, Y., & Zheng, D. Q. (2020). Heat shock drives genomic instability and phenotypic variations in yeast. *AMB Express*, *10*(1). https://doi.org/10.1186/s13568-020-01091-7

Stanley, D., Bandara, A., Fraser, S., Chambers, P. J., & Stanley, G. A. (2010). The ethanol stress response and ethanol tolerance of Saccharomyces cerevisiae. *Journal of Applied Microbiology*, *109*(1), 13–24.

Taddei, A., & Gasser, S. M. (2012). Structure and function in the budding yeast nucleus. *Genetics*, *192*(1), 107–129. https://doi.org/10.1534/genetics.112.140608

Tan, J. J. D., Ma, Z., Xie, Y., Yang, L., & Miao, Y. (2017). Quantitative analysis of actin filament assembly in yeast and plant by live cell fluorescence microscopy. *Micron*, *103*, 78–83. https://doi.org/10.1016/j.micron.2017.09.011

Triandafillou, C. G., Katanski, C. D., Dinner, A. R., & Allan Drummond, D. (2020). Transient intracellular acidification regulates the core transcriptional heat shock

response. *ELife*, *9*, e54880. doi: https://doi.org/10.7554/eLife.54880
Tye, B. W., & Churchman, L. S. (2021). Hsf1 activation by proteotoxic stress requires concurrent protein synthesis. *Molecular Biology of the Cell*, *32*(19), 1800–1806. https://doi.org/10.1091/mbc.E21-01-0014
Tye, B. W., Commins, N., Ryazanova, L. V., Wühr, M., Springer, M., Pincus, D., & Churchman, L. S. (2019). Proteotoxicity from aberrant ribosome biogenesis compromises cell fitness. *ELife*, *8*. https://doi.org/10.7554/eLife.43002
Verghese, J., Abrams, J., Wang, Y., & Morano, K. A. (2012). Biology of the Heat Shock Response and Protein Chaperones: Budding Yeast (Saccharomyces cerevisiae) as a Model System. *Microbiology and Molecular Biology Reviews*, *76*(2), 115–158. https://doi.org/10.1128/mmbr.05018-11
Voordeckers, K., Colding, C., Grasso, L., Pardo, B., Hoes, L., Kominek, J., Gielens, K., Dekoster, K., Gordon, J., Van der Zande, E., Bircham, P., Swings, T., Michiels, J., Van Loo, P., Nuyts, S., Pasero, P., Lisby, M., & Verstrepen, K. J. (2020). Ethanol exposure increases mutation rate through error-prone polymerases. *Nature Communications*, *11*(1), 3664. https://doi.org/10.1038/s41467-020-17447-3
Wendt, K. S., & Grosveld, F. G. (2014). Transcription in the context of the 3D nucleus. *Current Opinion in Genetics and Development*, *25*(1), 62–67. https://doi.org/10.1016/j.gde.2013.11.020
Zhang, H., Shao, S., Zeng, Y., Wang, X., Qin, Y., Ren, Q., Xiang, S., Wang, Y., Xiao, J., & Sun, Y. (2022). Reversible phase separation of HSF1 is required for an acute transcriptional response during heat shock. *Nature Cell Biology*, *24*(3), 340–352. https://doi.org/10.1038/s41556-022-00846-7
Zhao, J., Herrera-Diaz, J., & Gross, D. S. (2005). Domain-Wide Displacement of Histones by Activated Heat Shock Factor Occurs Independently of Swi/Snf and Is Not Correlated with RNA Polymerase II Density. *Molecular and Cellular Biology*, *25*(20), 8985–8999. https://doi.org/10.1128/mcb.25.20.8985-8999.2005
Zheng, X., Krakowiak, J., Patel, N., Beyzavi, A., Ezike, J., Khalil, A. S., & Pincus, D. (2016). Dynamic control of Hsf1 during heat shock by a chaperone switch and phosphorylation. *ELife*, *5*. https://doi.org/10.7554/eLife.18638

Tables

Table 1. Comparison of kinetics of heat shock and ethanol stress on *HSR* genes

Parameter	Heat Shock	Ethanol Stress
Hsf1 binding to UAS	Rapid, peak at 2.5 min	Slight delay, peak at 10 min
Pol II recruitment	Rapid, peak at 2.5 min	Severely delayed, detection starts at 10 min
Histone H3 occupancy	Rapid depletion	Transient increase, followed by gradual depletion
Genome compaction	Transient	Sustained
HSR gene transcription	Rapid	Delayed
HSR gene coalescence	Rapid, transient	Slightly delayed, transient
Hsf1 condensates	Rapidly induced, transient, well defined	Rapidly induced, stable, poorly defined